Computerized Medical Imaging and Graphics 113 (2024) 102355

Contents lists available at ScienceDirect

Computerized Medical Imaging and Graphics

journal homepage: www.elsevier.com/locate/compmedimag

Automatic artery/vein classification methods for retinal blood vessel: A review

Qihan Chen [a], Jianqing Peng [a,b,*], Shen Zhao [a,**], Wanquan Liu [a]

[a] School of Intelligent Systems Engineering, Shenzhen Campus of Sun Yat-sen University, Shenzhen 518107, China
[b] Guangdong Provincial Key Laboratory of Fire Science and Technology, Guangzhou 510006, China

ARTICLE INFO

Keywords:
Retinal arteriovenous classification
Deep learning
Topological graph

ABSTRACT

Automatic retinal arteriovenous classification can assist ophthalmologists in disease early diagnosis. Deep learning-based methods and topological graph-based methods have become the main solutions for retinal arteriovenous classification in recent years. This paper reviews the automatic retinal arteriovenous classification methods from 2003 to 2022. Firstly, we compare different methods and provide comparison tables of the summary results. Secondly, we complete the classification of the public arteriovenous classification datasets and provide the annotation development tables of different datasets. Finally, we sort out the challenges of evaluation methods and provide a comprehensive evaluation system. Quantitative and qualitative analysis shows the changes in research hotspots over time, Quantitative and qualitative analyses reveal the evolution of research hotspots over time, highlighting the significance of exploring the integration of deep learning with topological information in future research.

1. Introduction

RTINAL blood vessel computation technologies have gradually found applications in clinical diagnosis. Currently, its most widespread application is to assist in the diabetic retinopathy diagnosis (Boudegga et al., 2021; Morano et al., 2021). The University of Porto and Hospital de Braga jointly published a deep learning-based DR grading computer-aided diagnosis (CAD) system called "DR|GRADUATE" (Araújo et al., 2020). This system can provide lesion grades (R0-R4) for fundus images and assess the uncertainty of each result. IDx-DR is the world's first AI diagnostic device approved for diagnosing diabetic retinopathy (Abràmoff et al., 2016). It utilizes Convolutional Neural Networks (CNNs) to classify lesions in images and detect the positions of major anatomical structures. Similar systems, such as RetmarkerDR (Ribeiro et al., 2015) in Portugal and EyeArt (Rajalakshmi et al., 2018) in Canada, have undergone preliminary validation in local programs. Malena et al (Daich Varela et al., 2023). have highlighted the beneficial role of AI-based retinal detection technologies during the COVID-19 pandemic. However, the current methods exhibit shortcomings in the interpretability of disease diagnosis results.

The accurate arteriovenous segmentation method is an important way to improve the interpretability of CAD systems. Arteriovenous classification of fundus images is indispensable in the early diagnosis of diseases (Morano et al., 2021; Jia and Zhuang, 2021). Many diseases alter the structural characteristics of retinal vessels such as diameter, length, angle, and curvature (Aras and Nugroho, 2020; Vázquez et al., 2010a; Azegrouz et al., 2006; Cheung et al., 2011a). Furthermore, the impact of many diseases such as hypertension, and diabetes is asymmetric on the arteriovenous (Chen et al., 2022). Hypertension and diabetes can narrow the caliber of retinal arterioles (Chew et al., 2012a). Diabetic retinopathy can also lead to venular widening (Guan et al., 2006a; Salamat et al., 2019). Because retinal fundus images can achieve non-invasive examination of vascular structure (Mookiah et al., 2021; L Srinidhi et al., 2017), these structural changes can be reflected by the arteriolar-to-venular ratio (AVR) (Yan et al., 2021; Tramontan et al., 2008) of fundus images. The AVR can be calculated after arteriovenous classification (Miri et al., 2017), so it is significant to achieve accurate arteriovenous classification of retinal images (Abdulsahib et al., 2021).

Automatic arteriovenous classification by computer can efficiently assist ophthalmologists in the early diagnosis of retinal diseases (Abdulsahib et al., 2021). Manual classification of fundus vessels requires excessive time, and the number of professional ophthalmologists

* Corresponding author at: School of Intelligent Systems Engineering, Shenzhen Campus of Sun Yat-sen University, Shenzhen 518107, China.
** Corresponding author.
E-mail addresses: pengjq7@mail.sysu.edu.cn (J. Peng), zhaosh35@mail.sysu.edu.cn (S. Zhao).

https://doi.org/10.1016/j.compmedimag.2024.102355
Received 26 September 2023; Received in revised form 6 February 2024; Accepted 6 February 2024
Available online 16 February 2024
0895-6111/

is too scarce to meet clinical needs (Niemeijer et al., 2004; Hu et al., 2022). Due to the complicated vascular structure and the large number of images, incorrect labeling is prone to occur in clinical work (Sule, 2022). However, a small error in the classification may cause a large error in the AVR (Dashtbozorg et al., 2014). Therefore, it is necessary to provide an accurate and effective retinal arteriovenous automatic classification method.

However, retinal vascular arteriovenous automatic classification faces many problems and challenges. We give some examples in Fig. 1 and summarize the main challenges as follows:

1) Retinal image illumination imbalance and low contrast problems (L Srinidhi et al., 2017; Miri et al., 2017): Light imaging processes may cause uneven image brightness. The thickness of the blood vessel will affect its contrast with the background.
2) Dataset scarcity, label inconsistency (Morano et al., 2021; Hu et al., 2022): The retinal arteriovenous classification data labeling is difficult and time-consuming. Existing datasets are scarce, especially those with pixel-level arterial labeling. Moreover, the subjective judgment of different labels will lead to incorrect or inconsistent labels.
3) Neglect or misclassification of microvessels (Estrada et al., 2015a; Hu et al., 2021): Multi-scale characteristics of retinal vessels should be considered. Because tiny arteries and veins are more susceptible to changes in blood pressure but difficult to distinguish. Many classification methods will show a sharp decline in performance on small-scale vessels.
4) The imbalance of sample proportion (Hu et al., 2021): Only about 15% of the area in the fundus image is blood vessels. In particular, end-to-end vascular classification methods are challenging to classify pixels directly into arteries, veins, or backgrounds.
5) Deficiency of vascular topological connectivity (Chen et al., 2022, 2020; Luo et al., 2022): Many methods based on deep learning ignore topological connectivity. The lack of topological connectivity makes the same segment may present arteriovenous staggered distribution.
6) Irregularities in evaluation metrics (Morano et al., 2021; Chen et al., 2022): Performance values are difficult to reflect the merits of methods comprehensively. Differences in label types can result in different evaluation patterns. Moreover, the evaluation areas and levels selected for different articles are not uniform. At the same time, there is still a lack of quantitative evaluation indicators for vascular topological connectivity.

More and more reviews summarize different studies exploring the above challenges. Although more reviews have focused on retinal vascular segmentation (Fraz et al., 2012; Singh and Tiwari, 2019; Khan et al., 2019; Soomro et al., 2019; Chen et al., 2021), the retinal arteriovenous classification task has gradually gained attention. Mookiah et al (Mookiah et al., 2021)., Srinidhi et al (L Srinidhi et al., 2017)., and Abdulsahib et al (Abdulsahib et al., 2021). have summarized methods both on vascular segmentation and arteriovenous classification. Miri et al (Miri et al., 2017). compared retinal arteriovenous classification methods from a modeling perspective. This evaluation method avoids the inconsistency of evaluation metrics. Alam et al (Alam et al., 2021). reviewed the technical principles and clinical applications of arteriovenous classification in fundus photography, optical coherence tomography, and OCT angiography. YAN et al (Yan et al., 2021). focus on the advantages and disadvantages of related improved algorithms. Arnould et al. (2023). summarized the related research on the automatic extraction of microvascular parameters by artificial intelligence technology, some of which involved retinal arteriovenous classification.

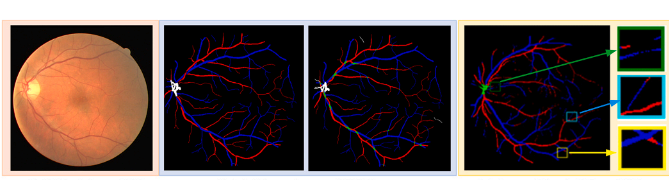
(a) Original image [90] (b) Label inconsistency [91][92] (c) Connectivity deficiency [18]

Fig. 1. Different Examples of Retinal Classification Challenges.

The existing reviews are deficient in two aspects. On the one hand, less attention has been paid to deep learning methods and topological graph methods. In particular, there has been no specific summary of the methods combining deep learning and topological information. However, these two methods are the mainstream ways to solve such problems in recent years. As shown in Table 1, Mookiah et al (Mookiah et al., 2021). have summarized the most articles on deep learning methods, while Yan et al (Yan et al., 2021). have compiled the most articles on topological graphs, with only 7 papers. On the other hand, the relevant datasets and evaluation methods have not been systematically reviewed. This paper supplements the deficiencies of the above research in these aspects.(Table 2–4)

(The columns labeled 'Time Range' and 'Auto CLS Methods' respectively record the time range and number of articles compiled by different reviews. 'DL' stands for the deep learning method, 'TG' for the topological graph method, and 'OT' for other methods. The columns labeled 'DS' and 'EV' indicate whether the article has included an arteriovenous classification dataset and evaluation method.).

This review focuses on the classification method based on deep learning and topological graphs. For completeness and to allow comparisons, we include other traditional methods. The following tasks are completed from literature collation and methods comparison.

1) Summarize the different approaches and their performance, and clarify the relationships between them.
2) Compile the public datasets for arteriovenous classification and their annotation improvement processes.
3) Summarize the shortcomings of existing evaluation systems and provide suggestions for improvement.
4) Identify current research gaps and future trends through qualitative and quantitative analysis.

The framework of this paper is as follows. Section 2 compares different methods of retinal arteriovenous classification. Section 3 summarizes the publicly available datasets related to retinal arteriovenous classification. Section 4 introduces the evaluation challenges and the multi-faceted evaluation system. Section 5 provides qualitative and quantitative analysis. Finally, the conclusion is drawn in Section 6.

Table 1
Retinal Arteriovenous Classification Reviews.

Paper Label	Time Range	Auto CLS Methods			DS	EV
		DL	TG	OT		
2017_Srinidhi_SEGCLS (L Srinidhi et al., 2017)	2009-2016	1	4	5	No	No
2017_Miri_CLS (Miri et al., 2017)	2003-2016	0	3	24	No	No
2020_Mookiah_SEGCLS (Mookiah et al., 2021)	2013-2020	7	5	15	No	No
2020_Alam_CLS (Alam et al., 2021)	2003-2018	6	6	26	No	No
2021_Yan _CLS (Yan et al., 2021)	2002-2019	0	7	18	No	No
2021_Abdulsahib_SEGCLS (Abdulsahib et al., 2021)	2003-2020	4	3	8	No	No
This paper	2003-2022	23	20	19	Yes	Yes

Table 2
Method Based on Other Methods.

Label	Source code	Method	Dataset	ACC	SE	SP	Comments
2003_Li_PG (Li et al., 2003)	**No info**	**Preprocessing**: No mention **Features**: Intensity features; Piecewise Gaussian model **Classifier**: Minimum Mahalanobis distance **Postprocessing**: No mention	Private dataset(NP)	_	_	_	**Advantages:** Utilizing a piecewise Gaussian model; emphasizing the central reflection of blood vessels. Employing a minimum Mahalanobis distance classifier to accomplish artery and vein classification. **Disadvantages:** Pre-segmentation of blood vessels is necessary. Validation has not been performed on a publicly available dataset.
2013_Relan_GMM (Relan et al., 2013)	**No info**	**Preprocessing**: Illumination correction; Contrast improvement **Features**: Color features **Classifier**: Gaussian Mixture Model Expectation-Maximization classifier **Postprocessing**: No mention	Private dataset(NP)	92.00	_	_	**Advantages:** Utilizing an unsupervised approach based on color features. Implementing repeated labeling verification through quadrant pairs. **Disadvantages:** The extraction of blood vessel centerlines requires manual annotation. Validation has not been performed on a publicly available dataset.
2021_Relan_GMM (Relan and Relan, 2021)	**No info**	**Preprocessing**: Homomorphic filtering; Multiscale line operator segmentation **Features**: Color features **Classifier**: Locally Consistent Gaussian Mixture Model **Postprocessing**: No mention	INSPIRE (544V_test_ALL_SEG_AV) INSPIRE (544V_test_ALL_SEG_A) INSPIRE (544V_test_ALL_SEG_V) VICAVR (732V_test_ALL_SEG_AV) VICAVR (732V_test_ALL_SEG_A) VICAVR (732V_test_ALL_SEG_V) MESSIDOR(NP) MESSIDOR(NP) MESSIDOR(NP)	90.65 _ _ 90.30 _ _ 93.80 _ _	_ 94.6 86.2 _ 90.7 89.8 _ 97.4 89.5	_ 86.2 94.6 _ 89.8 90.7 _ 89.5 97.3	**Advantages:** Utilizing a homomorphic filter for preprocessing to preserve strong contrast regions. Employing a local consistent Gaussian mixture model for unsupervised classification of retinal vessels; automatically selecting vessel and centerline pixels. **Disadvantages:** Only three main features are considered. There is potential for further improvement in classification performance.
2013_Mirsharif_LDA (Mirsharif et al., 2013)	**No info**	**Preprocessing**: Color normalization; Contrast improvement **Features**: Intensity, color features **Classifier**: LDA **Postprocessing**: Subtree correction	DRIVE(20/ 40_test_ALL_PIXEL_AV) Khatam(NP)	84.05 80.10	82.65 71.18	85.74 88.13	**Advantages:** Correcting mislabeling using the connectivity information of intersections and bifurcations. Integrating vessel tracking techniques and color information to classify the global vasculature. **Disadvantages:** Relatively limited validation dataset. The potential relationship between local information and global connectivity is not considered.
2018_Huang_FLDA (Huang et al., 2018b)	**No info**	**Preprocessing**: luminosity normalization **Features**: Genetic search feature selection **Classifier**: LDA **Postprocessing**: Segment-wise classification	DRIVE(20/ 40_test_ALL_PIXEL_AV) INSPIRE(20/ 40_test_ALL_PIXEL_AV)	72.00 90.20	70.90 89.60	73.80 91.30	**Advantages:** Extracting 455 features for each blood vessel centerline. Optimizing feature subsets using Genetic-search feature selection. **Disadvantages:** The large number of features and genetic search can lead to a significant computational time.
2018_Huang_LDA (Huang et al., 2018a)	**No info**	**Preprocessing**: Luminosity normalization **Features**: Lightness reflection features **Classifier**: LDA **Postprocessing**: No mention	INSPIRE(20/ 40_test_ALL_SEG_AV) VICAVR(10/ 58_test_ROI_SEG_AV) NIDEK(NP)	85.1 90.6 _	_ _ _	_ _ _	**Advantages:** Selection of 4 new features that reflect the brightness and reflection information of blood vessel contours. **Disadvantages:** Lack of consideration for global information and vascular connectivity.
2003_Grisan_DEI (Grisan and Ruggeri, 2003)	**No info**	**Preprocessing**: Illumination correction; Contrast improvement **Features**: Intensity features **Classifier**: Fuzzy clustering **Postprocessing**: No mention	Private dataset(NP)	_	_	_	**Advantages:** Dividing the fundus color image into four quadrants for separate processing. **Disadvantages:** Lack of consideration for global information, and a relatively small number of samples in the validation dataset.
2007_Kondermann_SVMNN (Kondermann et al., 2007)	**No info**	**Preprocessing**: Image enhancement; Skeleton extraction **Features**: Color, profile	Private dataset(NP)	_	_	_	**Advantages:** Utilizing both vessel contour features and color features. Improved performance through the combination of vessel segment knowledge and neural

(*continued on next page*)

Table 2 (*continued*)

Label	Source code	Method	Dataset	ACC	SE	SP	Comments
		features; PCA **Classifier**: SVM/NN **Postprocessing**: No mention					networks. **Disadvantages:** Requires pre-segmentation of vessels. Poorer classification performance for small vessel segments.
2009_Niemeijer_KNN (Niemeijer et al., 2009)	**No info**	**Preprocessing**: Vessel segment extraction **Features**: Width, angle, intensity, derivative features **Classifier**: KNN **Postprocessing**: Label unification	DRIVE(20/40_test_ALL_CT_AV)	_	_	_	**Advantages:** Considering collective features such as vessel width and angles. Taking global connectivity into account for correcting initial labels. **Disadvantages:** Some features may be irrelevant to the classification process. Common evaluation metrics are not used.
2010_Vázquez_kmeans (Vázquez et al., 2010b)	**No info**	**Preprocessing**: No mention **Features**: Color features **Classifier**: K-means **Postprocessing**: No mention	VICAVR(20/58_test_ROI_SEG_AV) VICAVR(58/58_test_ROI_SEG_AV)	86.53 86.34	_ _	_ _	**Advantages:** Three classification strategies based on the k-means algorithm were proposed. **Disadvantages:** The global connectivity of blood vessels has not been considered
2010_Vázquez_minpath (Vázquez et al., 2010c)	**No info**	**Preprocessing**: No mention **Features**: Color features **Classifier**: K-means **Postprocessing**: Minimal path approach	_	_	_	_	**Advantages:** Combining clustering and tracking algorithms. Incorporating color information through minimum path algorithm. **Disadvantages:** Validation has not been performed on a publicly available dataset.
2011_Vázquez_minpath (Vázquez et al., 2013)	**No info**	**Preprocessing**: No mention **Features**: Color feature **Classifier**: K-means **Postprocessing**: Minimal path approach; Voting system	_	_	_	_	**Advantages:** Merging vessel segments with different radii through tracking algorithms to ensure consistent classification. **Disadvantages:** Validation has not been performed on a publicly available dataset. Geometric structural information of blood vessels has not been taken into consideration.
2012_Saez_kmeans (Saez et al., 2012)	**No info**	**Preprocessing**: Profile extraction **Features**: Color features **Classifier**: K-means **Postprocessing**: No mention	Private dataset(NP)	_	_	_	**Advantages:** Diameter information of arteries and veins has been considered. **Disadvantages:** Validation has not been performed on a publicly available dataset. The blood vessel segmentation algorithm has not been validated.
2012_Zamperini_BF (Zamperini et al., 2012)	**No info**	**Preprocessing**: No mention **Features**: Color features; Spatial location; Vessel size **Classifier**: Linear Bayes **Postprocessing**: No mention	Private dataset(NP)	_	_	_	**Advantages:** Integrating color features, spatial positioning, and geometric information. **Disadvantages:** The lack of further analysis on why the width information of blood vessels did not optimize the results.
2014_Chhabra_NN (Chhabra and Bhushan, 2014)	**No info**	**Preprocessing**: Illumination correction; Centerline extraction **Features**: Color features **Classifier**: Neural Network **Postprocessing**: No mention	DRIVE(20/40_test_ALL_PIXEL_AV)	85.10	_	_	**Advantages:** The earliest research in this field involved the use of backpropagation neural networks. It required a small number of features. **Disadvantages:** The number of samples in the validation dataset is relatively small.
2016_Vijayakumar_SVM (Vijayakumar et al., 2016)	**No info**	**Preprocessing**: Illumination correction **Features**: features selected by Random Forests **Classifier**: SVM **Postprocessing**: No mention	VICAVR(29/58_test_ROI_SEG_AV)	92.40	90.87	94.82	**Advantages:** Utilizing random forests to select optimal features for use as inputs to the SVM classifier. **Disadvantages:** The validation dataset is relatively small. The impact of preprocessing methods has not been thoroughly investigated.
2017_XU_KNN (Xu et al., 2017)	**No info**	**Preprocessing**: Intra-image regularization; Inter-subject normalization **Features**: Texture features; Color features **Classifier**: KNN **Postprocessing**: No mention	DRIVE(20/40_test_ALL_CT_AV)	92.90	91.50	92.90	**Advantages:** Joint consideration of color features and texture features. **Disadvantages:** The algorithm's performance under low-resolution images has not been considered. The continuity of blood vessels cannot be assured.
2020_Sun_SqStr (Sun et al., 2020)	**No info**	**Preprocessing**: FA image registration	Duke dataset(NP) Private dataset(NP)	91.00 92.00	89.00 89.00	93.00 94.00	**Advantages:** Combining the sequential growth information and structural

(*continued on next page*)

Table 2 (*continued*)

Label	Source code	Method	Dataset	ACC	SE	SP	Comments
		Features: FA sequence features; Vessel structural features **Classifier**: FCM; SVM **Postprocessing**: Seed region growth strategy					features of fluorescein angiography images to accomplish blood vessel classification. **Disadvantages:** High data quality requirements. Manual selection of the optic disc area is required.
2021_Irshad_OOBJ+SVM23 (Vijayakumar et al., 2016)	**No info**	**Preprocessing**: No mention **Features**: features selected by Binary Particle Swarm Optimization **Classifier**: SVM **Postprocessing**: No mention	INSPIRE(20/40_test_ALL_CT_AV) VICAVR(29/58_test_ROI_SEG_AV) Private dataset(NP)	94.61 91.92 92.70	_ _ _	_ _ _	**Advantages:** Using binary particle swarm optimization algorithm to select the optimal vascular features. The objective function considers both the size and correlation of the feature subset. **Disadvantages:** Lack of consideration for classifier optimization.

(The "Label" shows the paper's author, publication year, and category. The "Method" includes pre-processing techniques, selected features, classifiers, and post-processing methods. In the "Dataset" column, each dataset is followed by some tags. "NP" denotes unpublished datasets, "20/40_test" denotes the number of images used for testing evaluation, and "544V_test" represents the number of vessel segments used for testing evaluation since some methods evaluate vessel segments as the evaluation unit. "ALL" and "ROI" denote whether the entire image or ROI region was selected for evaluation. "SEG," "PIXEL," and "CT" represent the evaluation level of vessel segments, vessel pixels, and centerline pixels, respectively. "AV," "A," and "V" represent the evaluated objects, including arteries and veins, arteries only, and veins only. Finally, the selected performance metrics include ACC (accuracy), SEN (sensitivity), and SPE (specificity). The missing data is represented by "_".)

2. Clinical applications of retinal artery and vein classification

Accurate classification of retinal arteries and veins is the foundation for precise quantitative analysis. Structural changes in retinal vessels are associated with many diseases. The impact of these diseases on the structure of arteries and veins is asymmetrical. In particular, the structural changes in these retinal microvessels are likely to be early features of diseases. Therefore, quantitative analysis of structural changes in arteries and veins can play a crucial role in the prevention and diagnosis of related diseases. The prerequisite for structural quantification analysis is accurately classifying arteries and veins.

2.1. Diabetic retinopathy

Accurate artery and vein segmentation is crucial for the early diagnosis of diabetes. Microaneurysms, retinal hemorrhages, and exudates are representative signs of diabetic retinopathy, but these symptoms often occur in the later stages of diabetes. Research indicates that early signs of diabetes primarily manifest in specific changes in the diameter of the retinal small blood vessels.

Silva et al (da Silva et al., 2015). employed quantitative analysis of venous dilation in the upper temporal quadrant of diabetic patients, suggesting that microvascular changes can be used for early diagnosis of diabetes. In the early stages of diabetes, there is an increase in blood flow in the veins in the upper temporal quadrant, leading to the widening of small veins, resulting in a decrease in the diameter ratio of small arteries to small veins (Guan et al., 2006b).

Compared to existing diagnostic systems, artery and vein classification is more conducive to the early diagnosis and prevention of diabetes. Current diabetic retinopathy detection systems mainly rely on the diagnosis of symptoms in the middle and later stages. However, through accurate classification of arteries and veins followed by diameter analysis of the relevant vessels, diabetic retinopathy can be diagnosed earlier.

2.2. Cardiovascular diseases

The ratio of artery to vein width is associated with cardiovascular diseases, such as hypertension, which can asymmetrically impact the morphology of retinal arteries and veins (Chew et al., 2012b). Wong et al. indicate a correlation between the narrowing of retinal arterioles and the risk of female coronary heart disease (Wong et al., 2001, 2002), while focal arteriolar narrowing is significantly associated with elderly hypertension (Guan et al., 2006b; Wong et al., 2003). Research by Smith et al (Smith et al., 2004). suggests that structural changes in retinal vessels may precede the onset of severe hypertension, making it useful for the diagnosis and prevention of severe hypertension.

Calculating the artery-vein width ratio can assess the risk of related diseases, and accurate artery and vein classification is a fundamental step in calculating the arteriovenous ratio.

2.3. Other diseases

Several diseases require the classification of arteries and veins for diagnostic analysis, such as retinopathy of prematurity and familial retinal arteriolar tortuosity.

Retinopathy of prematurity refers to abnormal dilation and tortuosity of the retinal vessels near the optic disc in the posterior part of the retina in premature infants. Cheung et al (Cheung et al., 2011b). quantitatively analyzed the morphological changes in arteries and veins caused by retinopathy of prematurity. The results indicate that the structural differences are mainly manifested in the tortuosity of small arteries, while the tortuosity curvature of veins does not show significant differences. Familial retinal arteriolar tortuosity is a rare autosomal dominant inherited disease (Sutter and Helbig, 2003), characterized by affecting the tortuosity of retinal arterioles. In the later stages, it may lead to retinal hemorrhage, emphasizing the importance of early diagnosis.

Currently, the diagnosis and analysis of these diseases are done manually. Existing computer-assisted software can assist in completing relevant structural parameters but cannot automatically differentiate between arteries and veins. Particularly, the differentiation of arteries and veins in some small vessels is challenging, and inexperienced doctors may struggle to accomplish it.

3. Retinal vessel artery/vein automatic classification methods

In this section, we review the automatic classification method of retinal vessels. we divide retinal arteriovenous classification methods into traditional methods, topological graph-based methods, and deep learning-based methods, as show in Fig. 2.

The topological graph method can utilize the structural characteristics of retinal vessels. It solves the problem of vascular connectivity. Deep learning methods can achieve end-to-end vascular classification. It solves the problem that the classification results of traditional methods are strongly dependent on the segmentation results. Therefore, we have

Table 3
Method Based on Topological Graph.

Label	Source	Method	Dataset	ACC	SE	SP	Comments
2007_Rothaus_TUG (Rothaus et al., 2007)	No info	Preprocessing: Graph construction Features: Graph feature representation Classifier: AC-3 algorithm Postprocessing: No mention	DRIVE(_)	_	_	_	Advantages: Rule-based method for blood vessel image classification. Disadvantages: Initial manual labeling is required.
2009_Lin_TUG+KM (Lin et al., 2009)	No info	Preprocessing: Graph construction Features: Direction, width, color feature; Graph feature representation Classifier: Kalman filter Postprocessing: No mention	DRIVE(5/40_test_ALL_SEG_AV)	92.10	_	_	Advantages: Iteratively connecting vessel segments using a Kalman filter to optimize the topological continuity of blood vessels. Disadvantages: The validation dataset is relatively small.
2009_Rothaus_TUG+AC3 (Rothaus et al., 2009)	No info	Preprocessing: Graph construction Features: Graph feature representation Classifier: AC-3 algorithm Postprocessing: No mention	STARE(_) DRIVE(_)	_ _	_ _	_ _	Advantages: Formulating the blood vessel classification problem as a dual-constraint search problem. Disadvantages: Pre-segmentation of the blood vessel and initial manual labeling are required.
2013_Dashtbozorg_TUG (Dashtbozorg et al., 2013)	No info	Preprocessing: Graph construction Features: Intensity feature; Graph feature representation Classifier: LDA Postprocessing: No mention	INSPIRE(_)	_	_	_	Advantages: Integrating structural information of blood vessels with color features. Correcting common linking errors in the process. Disadvantages: Assuming a constant diameter for all optic disks. Structural constraints only consider common types.
2013_Lau_TUG (Lau et al., 2013)	No info	Preprocessing: Graph construction Features: Graph feature representation Classifier: Graph Tracer Postprocessing: No mention	Private dataset(NP)	_	_	_	Advantages: Transforming the blood vessel segment classification problem into an optimization problem of finding the optimal forest in the graph. Incorporating the correction of linking errors using intersection points and bifurcation points. Disadvantages: Validation has not been performed on a publicly available dataset.
2014_Dashtbozorg_TUG (Dashtbozorg et al., 2014)	No info	Preprocessing: Intensity normalization; Graph construction Features: Intensity feature; Graph feature representation Classifier: LDA Postprocessing: No mention	INSPIRE(40/40_test_ALL_CT_AV) INSPIRE(40/40_test_ALL_PIXEL_AV) INSPIRE(40/40_test_ROI_CT_AV) INSPIRE(40/40_test_ROI_PIXEL_AV) DRIVE(20/40_test_ROI_CT_AV) VICAVR(58/58_test_ALL_SEG_AV)	84.90 88.30 95.90 91.10 87.40 89.80	_ _ _ _ _ _	_ _ _ _ _ _	Advantages: Assigning initial labels to edges in the graph based on node types. Completing the final classification by combining initial labels with color intensity features. Completed a relatively comprehensive validation. Disadvantages: Not considering uncommon node types. Local errors may impact the overall results.
2014_Joshi_DJ (Joshi et al., 2014)	No info	Preprocessing: Graph construction Features: Orientation, width, intensity feature; Graph feature representation Classifier: Fuzzy C-means clustering Postprocessing: No mention	EYECHECK(NP)	_	_	_	Advantages: Utilizing Dijkstra's algorithm to find the optimal path based on blood vessel intensity, direction, and width information. Disadvantages: Validation has not been performed on a publicly available dataset.
2015_Divya_TUG+KNN (Divya, 2015)	No info	Preprocessing: Graph construction Features: Intensity feature; Graph feature representation Classifier: KNN Postprocessing: No mention	_	_	_	_	Advantages: Obtaining initial labels based on node types and vessel intensity information, then utilizing KNN for the final classification. Disadvantages: The method has not undergone validation.
2015_Hu_TUG+SVM (Hu et al., 2015)	No info	Preprocessing: Graph construction Features: Direction,	DRIVE(20/40_test_ALL_PIXEL_AV)	86.11 85.91	_ _	_ _	Advantages: Obtaining a vessel potential connectivity map through local information. Correcting local

(*continued on next page*)

Table 3 (*continued*)

Label	Source	Method	Dataset	ACC	SE	SP	Comments
		width, intensity, orientation feature; Graph feature representation Classifier: SVM; Graph-based metaheuristic algorithm Postprocessing: No mention	DRIVE(20/40_test_ALL_CT_AV)				errors through metaheuristic learning. Disadvantages: The algorithm has a relatively long computational time. Inability to handle graphs that contain cycles.
2018_Pellegrini_TUC+LBC (Pellegrini et al., 2018)	No info	Preprocessing: Graph construction Features: Intensity, morphology feature; Graph feature representation Classifier: Linear Bayesian classifier (LBC) Postprocessing: Graph cut approach.	WIDE(30/30_test_ALL_SEG_AV) ZONE-C(NP) TASCFORCE(NP)	86.40 86.50 88.30	_ _ _	_ _ _	Advantages: The first application of Bayesian classifiers and graph cuts for Ultra-Wide Field of View-SLO images. Disadvantages: Graph cuts do not sufficiently consider certain node types.
2018_Zhao_TUG_VETO1 (Zhao et al., 2018)	No info	Preprocessing: Graph construction Features: Intensity, morphology feature; Graph feature representation Classifier: Dominant set clustering Postprocessing: No mention	INSPIRE(40/40_test_ALL_CT_AV) DRIVE(20/40_test_ALL_PIXEL_AV) VICAVR(58/58_test_ALL_CT_AV)	91 _ 91.0	91.8 91.9 _	90.2 91.5 _	Advantages: Successfully applied dominant sets clustering to blood vessel classification. The relevant dataset has been made publicly available. Disadvantages: The classification results depend on the pre-segmentation of blood vessels.
2019_Srinidhi_TUG+RF (Srinidhi et al., 2019)	No info	Preprocessing: Graph construction; Keypoints identification Features: Intensity, morphology feature; Graph feature representation Classifier: Random forest classifier Postprocessing: No mention	DRIVE(20/40_test_ALL_PIXEL_AV) DRIVE(20/40_test_ALL_CT_AV) INSPIRE(20/40_test_ALL_CT_AV) WIDE(15/30_test_ALL_CT_AV)	94.7 93.2 96.8 90.2	96.6 95.0 96.9 92.3	92.9 91.5 96.6 88.2	Advantages: Partitioning subtrees based on local features such as vessel intensity and morphology. Considering global information for further subdivision into arteries and veins. Innovatively considering curvature features. Disadvantages: The performance of this method is suboptimal in wide-field images.
2020_Zhao_TUG_VETO2 (Zhao et al., 2020)	(Homepage of Yitian Zhao,)	Preprocessing: Graph construction Features: Intensity, morphology feature; Graph feature representation Classifier: Dominant set clustering Postprocessing: No mention	INSPIRE(20/40_test_ALL_CT_AV) DRIVE(20/40_test_ALL_SEG_AV) VICAVR(58/58_test_ALL_SEG_AV) WIDE(30/30_test_ALL_CT_AV)	96.4 93.5 94.6 95.2	96.8 94.2 95.4 96.2	95.7 92.7 93.8 94.2	Advantages: Establishing topological estimation and AV classification as a pairwise clustering problem. The classification process emphasizes the consideration of topological properties. The method has undergone thorough validation. Disadvantages: The classification results depend on the pre-segmentation of blood vessels.
2015_De_TDG+W (De et al., 2016)	No info	Preprocessing: Direct graph construction Features: Direct graph feature representation Classifier: Label propagation Postprocessing: No mention	_	_	_	_	Advantages: make the connection between the tracing problem and the digraph matrix-forest theorem in algebraic graph theory for the first time Disadvantages: The method is not specifically designed for retinal artery-vein classification.
2015_Estrada_TTE (Estrada et al., 2015a)	No info	Preprocessing: Direct graph construction Features: Direct graph feature representation Classifier: Likelihood model; Best-first search Postprocessing: No mention	WIDE(15/30_test_ALL_SEG_AV) DRIVE(20/40_test_ALL_SEG_AV) DRIVE(20/40_test_ALL_CT_AV) INSPIRE(20/40_test_ALL_SEG_AV)	91.0 93.5 91.7 90.9	91.0 93.0 91.7 91.2	90.9 94.1 91.7 90.2	Advantages: Completing artery-vein classification through mapping and probability propagation. Disadvantages: There may be an issue of inconsistency in artery-vein types for some blood vessels across frames.
2015_Estrada_TTE+WIDE (Estrada et al., 2015b)	No info	Preprocessing: Direct graph construction Features: Direct graph feature representation Classifier: Heuristic search algorithm Postprocessing: No mention	WIDE(15/30_test_ALL_SEG_AV)	_	_	_	Advantages: Using heuristic search to achieve topological estimation of tree structures. Disadvantages: The validation dataset is relatively small.
2016_Lyu_TDG+CO (Xingzheng et al., 2016)	No info	Preprocessing: Direct graph construction Features: Direct graph	DRIVE(20/40_test_ALL_CT_AV)	83.21 _	78.05 _	87.42 _	Advantages: Dividing the vascular tree by clustering based on curvature direction. Correcting misconnections

(*continued on next page*)

Table 3 (*continued*)

Label	Source	Method	Dataset	ACC	SE	SP	Comments
		feature representation Classifier: Curvature orientation clustering Postprocessing: No mention	INSPIRE(20/ 40_test_ALL_CT_AV)				based on prior knowledge of curvature. Disadvantages: There may be instances where partial connections are disrupted.
2017_De_TDG+W (De et al., 2018)	No info	Preprocessing: Direct graph construction Features: Direct graph feature representation Classifier: Absorbing Random Walks Postprocessing: No mention	DRIVE(20/ 40_test_ALL_SEG_AV)	_	_	_	Advantages: A novel random walk approach on directed graphs using absorbing Markov chains. The algorithm is simple and easy to implement. Disadvantages: The validation dataset is relatively small. There are errors in predicting the direction of some blood vessels.
2019_Martinez-Perez_DG (Martinez-Perez et al., 2020)	No info	Preprocessing: Direct graph construction Features: Direct graph feature representation; Color feature Classifier: Fuzzy C-means clustering Postprocessing: No mention	Private dataset(NP)	79.00	83.00	74.00	Advantages: Identifying vessel bifurcations and intersections based on direction and local geometric information. Using color information for fuzzy logic classification in artery-vein classification. Disadvantages: Validation has not been performed on a publicly available dataset.
2019_Zhao_TDG (Zhao et al., 2019)	No info	Preprocessing: Direct graph construction Features: Direct graph feature representation; Morphology feature Classifier: Label propagation Postprocessing: Competition principle	HRF(_)	_	_	_	Advantages: Establishing a directed graph and quantifying relevant parameters. Solving the artery-vein classification problem using parent-child relationships. Disadvantages: Quantitative analysis was not presented.

summarized the two mainstream methods and collated traditional methods for comparison.

Traditional methods include linear discriminant analyzer (LDA), Gaussian Model, and traditional machine learning methods. The topology graph method is divided into undirected graphs and directed graphs. Deep learning-based methods are divided into convolutional neural networks (CNN), generative adversarial networks (GAN), and graph neural networks (GNN).

We discussed each category and summarized the papers in Table 2, 3 and 4. The tables specify labels, methods, validation databases, and performance for each paper entry.

3.1. Overview

There are five main steps for the retinal blood vessel classification task (Miri et al., 2017; Abdulsahib et al., 2021). (1) Pre-processing, including data augmentation and vessel segmentation. (2) Classification region selection, common regions include the ROI region and the whole image. (3) Feature extraction, including color features, topological features, depth features, etc. (4) Feature classification, classify the feature vectors extracted in the previous step. (5) Post-processing, which mainly ensures the consistency of labels for a particular vessel segment or vessel subtree. The method of the pre-processing stage has been well-established. Iqbal et al (Iqbal et al., 2022). have made a comprehensive summary. The subsequent discussion of this section will not involve methods of pre-processing.

3.2. Traditional methods

The traditional methods commonly used for retinal arteriovenous classification include linear discriminant analyzer (LDA), Gaussian model, and traditional machine learning methods. Some articles explore the performance of different classifiers, while some study the effect of feature selection on the classification algorithm.

3.2.1. Linear discriminant analyzer

LDA is one of the commonly used non-machine learning feature classifiers.

Mirsharif et al (Mirsharif et al., 2013). studied pixel-level features and the performance of different classifiers. LDA is chosen as the best classifier for their method. They obtained the vessel segments by vessel skeleton extraction and removing the intersections and bifurcations. They further divided the vessel segments into smaller subsets. After that, they integrated tracking technology and color information to classify the global blood vessels.

Huang et al (Huang et al., 2018a, 2018b). also utilized the LDA classifier to classify features but focused on feature selection techniques. In (Huang et al., 2018a), they explored a feature extraction method based on the contour brightness information and reflection features of retinal arteries and veins. In (Huang et al., 2018b), they proposed a genetic search-based feature selection approach. By extracting a wide range of features, they determine the optimal feature subset for classification using the genetic search algorithm.

3.2.2. Gaussian model

The Gaussian model can be used to describe features, and can also be used to classify features.

Li et al (Li et al., 2003). proposed a piecewise Gaussian model to describe the intensity distribution of vessel profile, which considered the difference between the central reflection of the retinal artery and vein. Finally, a minimum Mahalanobis distance classifier was used for classification.

Relan et al (Relan et al., 2013). employed the GMM-EM (Gaussian mixture model, expectation maximization) unsupervised classifier and a quadrant pairing method based on color features to automatically classify retinal vessels. In their recent work (Relan and Relan, 2021), they expanded on this unsupervised approach. They first applied homomorphic filtering for pre-processing and denoising. They then achieved vessel segmentation using unsupervised multiscale line operator segmentation. Finally, they utilized the Locally Consistent Gaussian

Table 4
Method Based on Deep Learning.

Label	Source	Method	Dataset	ACC	SE	SP	Comments
2017_Girard_CNN+LSP (Girard and Cheriet, 2017)	**No info**	**Preprocessing**: Contrast-enhancement; Data augmentation **Features:** CNN feature representation **Classifier:** Softmax **Postprocessing:** Likelihood score propagation	DRIVE(20/40_test_ALL_PIXEL_AV) DRIVE(20/40_test_ALL_CT_AV) MESSIDOR(NP)	86.00 95.40 96.60	92.30 93.60 90.60	93.10 93.10 91.80	**Advantages:** Utilizing CNN to obtain initial scores for arteries and veins, then obtaining the classification results through graph propagation of probability scores. **Disadvantages:** The blood vessels are pre-segmented. Structural information of blood vessels has not been considered.
2017_Welikala_CNN (Welikala et al., 2017)	**No info**	**Preprocessing**: Intensity transformation **Features:** CNN feature representation **Classifier:** RELU **Postprocessing**: No mention	DRIVE(15/40_test_ALL_PIXEL_AV) DRIVE(15/40_test_ALL_SEG_AV) DRIVE(15/40_test_ROI_PIXEL_AV) DRIVE(15/40_test_ROI_SEG_AV) UK Biobank(NP)	91.97 91.27 91.99 90.77	_ _ _ _	_ _ _ _	**Advantages:** Using convolutional neural networks to perform classification on small pixel blocks. Then a voting strategy to complete the artery-vein classification for the entire vessel segment. **Disadvantages:** This method is overly sensitive to small pixel variations.
2019_Galdran_UNET+UA (Galdran et al., 2019)	**(**GitHub - agaldran/a_v_uncertain: Code for our ISBI, paper on Artery/Vein classification with uncertainty predictions, 2019, **)**	**Preprocessing**: Illumination correction; Color transfer **Features:** FCN feature representation using U-Net **Classifier:** Sigmoid **Postprocessing:** No mention	DRIVE(20/40_test_ALL_PIXEL_AV) INSPIRE(40/40_test_ALL_CT_AV) LES-AV(22/22_test_ALL_PIXEL_AV)	89.00 80.00 86.00	89.00 82.00 88.00	90.00 78.00 85.00	**Advantages:** The focus is on uncertain blood vessels. Pixel-level classification is not dependent on pre-segmentation. **Disadvantages:** There is no detailed explanation of the evaluation for uncertain vessel types.
2019_Girard_CNN+LSP (Girard et al., 2019)	**No info**	**Preprocessing**: Contrast-enhancement; Data augmentation **Features:** CNN feature representation **Classifier:** Softmax **Postprocessing:** Likelihood score propagation	DRIVE(20/40_test_ALL_PIXEL_AV) DRIVE(20/40_test_ALL_CT_AV) MESSIDOR(NP)	86.50 _	86.30 93.70	86.60 92.90	**Advantages:** Simulating natural blood flow through probability score propagation to introduce global information. Computation has a low cost and is fast. **Disadvantages:** Vascular intersections and uncertain vessel types have not been taken into consideration.
2019_Hemelings_UNET (Hemelings et al., 2019)	**(**GitHub - rubenhx/av-segmentation,**)**	**Preprocessing**: Gaussian filter; Normalization **Features:** FCN feature representation using U-Net **Classifier:** Softmax **Postprocessing**: No mention	DRIVE(20/40_test_ALL_PIXEL_AV) DRIVE(20/40_test_ALL_CT_AV) DRIVE(20/40_test_ROI_PIXEL_AV) DRIVE(20/40_test_ROI_CT_AV) HRF(15/45_test_ALL_PIXEL_AV) HRF(15/45_test_ALL_CT_AV)	93.86 91.90 94.42 91.59 96.81 79.92	94.87 94.66 96.17 95.81 _ _	93.02 89.42 92.84 87.57 _ _	**Advantages:** Firstly proposed a deep learning architecture for simultaneous vascular extraction and artery/vein identification. A comprehensive evaluation has been conducted. **Disadvantages:** There is an issue of connectivity loss in small vessels.
2019_Ma_UNET+SAM (Ma et al., 2019)	**No info**	**Preprocessing**: Illumination correction; Vessel enhancement **Features:** FCN feature	DRIVE(20/40_test_ALL_PIXEL_AV) INSPIRE(40/40_test_ALL_CT_AV)	94.50 91.60	93.40 92.40	95.50 91.30	**Advantages:** Integrated preprocessing knowledge and vessel enhancement techniques at the input end. The network's

(*continued on next page*)

Table 4 (*continued*)

Label	Source	Method	Dataset	ACC	SE	SP	Comments
		representation using U-Net **Classifier**: Sigmoid **Postprocessing**: No mention					output end incorporates a spatial activation mechanism. **Disadvantages:** Pixel-level validation has not been conducted. The topological connectivity of blood vessels has not been considered.
2020_Hu_VCNET (Hu et al., 2021)	**No info**	**Preprocessing**: No mention **Features**: FCN feature representation using U-Net; Vessel-Constraint module; Gaussian activation function **Classifier**: Sigmoid **Postprocessing**: No mention	DRIVE(20/ 40_test_ALL_PIXEL_AV) LES-AV(11/ 22_test_ALL_PIXEL_AV) HRF(30/ 45_test_ALL_PIXEL_AV) Tongren(NP) Kailuan(NP)	95.54 94.46 96.46 94.68 94.42	93.60 94.25 95.88 94.21 94.13	97.48 94.67 97.04 95.16 94.72	**Advantages:** Considered vessel edge information through the vessel constraint module. Considered vessel information at different scales using a multi-scale module. **Disadvantages:** Unable to handle large-scale fundus images. High computational resource requirements.
2020_Li_UNET+PP (Li et al., 2020b)	(GitHub - conscienceli/SeqNet)	**Preprocessing**: No mention **Features**: FCN feature representation using U-Net **Classifier**: Softmax **Postprocessing**: Intra-segment Label Unification; Inter-segment Prediction Propagation	DRIVE(20/ 40_test_ALL_PIXEL_AV) DRIVE(20/ 40_test_ALL_CT_AV) LES-AV(11/ 22_test_ALL_PIXEL_AV) LES-AV(11/ 22_test_ALL_CT_AV)	96.70 91.90 97.80 87.40	_ _ _ _	_ _ _ _	**Advantages:** Utilizing a U-Net architecture to address both segmentation and classification problems in tandem. Combining vascular structural information for post-processing to ensure connectivity. **Disadvantages:** The algorithm has high complexity and computational costs.
2020_Li_UNET+TRC (Li et al., 2020a)	**No info**	**Preprocessing**: Haze-removal technique **Features**: FCN feature representation using U-Net **Classifier**: No mention **Postprocessing**: Tracking algorithm	Private dataset(NP)	93.57	96.23	91.16	**Advantages:** Optimizing neural network segmentation results using vascular tracking techniques. **Disadvantages:** Validation has not been performed on a publicly available dataset.
2021_Morano_UNET+LOSS (Morano et al., 2021)	**No info**	**Preprocessing**: Contrast enhancement; Intensity normalization **Features**: FCN feature representation using U-Net **Classifier**: Sigmoid **Postprocessing**: No mention	DRIVE(20/ 40_test_ALL_PIXEL_AV)	89.24	87.47	90.89	**Advantages:** Proposing an advanced error function that enables the decomposition of joint tasks. Establishing three separate classification tasks to preserve the connectivity of blood vessels. **Disadvantages:** There are still a few noticeable prediction errors in the results. The validation dataset is relatively small.
2021_Shin_UNET+TOOP (Shin et al., 2020)	(syshin, 1014, 2020)	**Preprocessing**: **Features**: FCN feature representation using U-Net; Graph representation feature **Classifier**: No mention **Postprocessing**: Tree tracing;	DRIVE(20/ 40_test_ALL_CT_AV) IOSTAR(9/ 18_test_ALL_CT_AV) IOSTAR(9/ 18_test_ALL_SEG_AV)	91.40 70.70 76.50	90.90 72.30 78.40	91.80 69.20 74.20	**Advantages:** Transforming vascular topology estimation into deep learning-based pairwise classification. Combining a voting mechanism significantly ensures the topological connectivity of blood vessels.

(continued on next page)

Table 4 (*continued*)

Label	Source	Method	Dataset	ACC	SE	SP	Comments
		Tree-wise class voting					**Disadvantages:** Vascular iteration starts from the terminals, and errors may occur when multiple junctions are encountered.
2022_Khanal_UNET+TDG (Khanal et al., 2022)	**No info**	**Preprocessing**: No mention **Features**: FCN feature representation using U-Net; Directed graph representation feature **Classifier**: Topology Estimation **Postprocessing**: High-Level Graph Operations	_	_	_	_	**Advantages:** Correcting the Unet segmentation results using a directed graph and advanced operations. **Disadvantages:** Validation has not been performed on a publicly available dataset. High-level operations can only correct common types.
2022_Chowdhury_UNET+ATTEN (Chowdhury et al., 2022)	**No info**	**Preprocessing**: No mention **Features:** multiscale feature representation using MSGANet-RAV **Classifier:** No mention **Postprocessing**: No mention	DRIVE(20/40_test_ALL_PIXEL_AV) LEI-CENTRAL(NP)	95.48 93.15	93.59 92.17	97.27 94.13	**Advantages:** Using an encoder to extract multi-scale features. The self-attention module in the decoder can incorporate contextual information. **Disadvantages:** Changes in brightness and uneven illumination can lead to a decrease in algorithm performance.
2020_Garifullin_BDL+UC (Garifullin et al., 2020)	**No info**	**Preprocessing**: Contrast enhancement; Channel normalization **Features**: FCN feature representation using DenseFCN **Classifier**: Sigmoid **Postprocessing**: No mention	DRIVE(20/40_test_ALL_PIXEL_A) DRIVE(20/40_test_ALL_PIXEL_V)	96.80 96.60	63.60 75.20	98.80 98.20	**Advantages:** Using Bayesian deep learning methods to address prediction problems when class labels are unavailable. **Disadvantages:** The impact of preprocessing results on label quantization has not been discussed. Vascular connectivity has not been considered.
2020_Chen_TRGAN (Chen et al., 2020)	**No info**	**Preprocessing**: Shuffle the ground-truth mask **Features**: FCN feature representation using U-Net; Topology Ranking GAN **Classifier**: No mention **Postprocessing**: No mention	DRIVE(20/40_test_ALL_PIXEL_AV) INSPIRE(40/40_test_ALL_CT_AV)	96.29 93.40	95.28 89.05	97.14 97.29	**Advantages:** Optimizing the connectivity of predicted results by ranking them through a discriminator based on topological connectivity. **Disadvantages:** Only qualitative sorting has been performed, lacking a study on quantitative parameters.
2020_Yang_topGAN (Yang et al., 2020)	**No info**	**Preprocessing**: Adaptive histogram equalization; Morphologic bottom-hat transformation **Features**: FCN feature representation using U-Net; Topology-Aware GAN **Classifier**: No mention **Postprocessing**: Refinement model	DRIVE(20/40_test_ALL_PIXEL_AV) CVDG(NP)	94.30 _	93.00 _	91.80 _	**Advantages:** Completing the classification of retinal arteries and veins using GANs with topological structure constraints and adversarial loss. **Disadvantages:** There are prediction errors on small-sized vessels. The validation dataset is relatively small.

(continued on next page)

Table 4 (*continued*)

Label	Source	Method	Dataset	ACC	SE	SP	Comments
2021_Chen_TWGAN (Chen et al., 2022)	(GitHub - o0t1ng0o/TW-GAN)	**Preprocessing**: Shuffle the ground-truth mask; Dilate the ground-truth mask **Features**: FCN feature representation using U-Net; Topology Ranking GAN; Width-aware module **Classifier**: No mention **Postprocessing**: No mention	DRIVE(20/ 40_test_ALL_PIXEL_AV) DRIVE(20/ 40_test_ALL_CT_AV) INSPIRE(40/ 40_test_ALL_CT_AV) HRF(15/ 45_test_ALL_PIXEL_AV) HRF(15/ 45_test_ALL_CT_AV)	96.34 86.63 82.21 96.50 89.82	95.38 88.71 83.30 97.01 92.19	97.2 84.99 81.49 96.14 87.68	**Advantages:** First time incorporating topological connectivity and width information into a deep learning framework. Released new annotations for the HRF dataset. **Disadvantages:** Lacks quantitative research on topological connectivity.
2022_Hu_GAN+MS+Toop+S (Hu et al., 2022)	(TwistedW, 2023)	**Preprocessing**: Data augmentation **Features**: Multi-Scale feature extracted from CNN; Sample Re-Weighting; A/V Discriminator **Classifier**: Sigmoid **Postprocessing**: No mention	DRIVE(20/ 40_test_ALL_PIXEL_AV) HRF(15/ 45_test_ALL_PIXEL_AV) LES-AV(11/ 22_test_ALL_PIXEL_AV) Private dataset(NP)	97.82 96.91 97.79 98.18	98.99 97.29 97.11 97.26	98.57 97.98 96.68 93.93	**Advantages:** The encoder incorporates a multi-scale transformation module, achieving the fusion of positional and semantic information. A sample re-weighting strategy is employed to mitigate the impact of noisy samples. **Disadvantages:** Post-processing methods for classification results have not been considered.
2022_Luo_TRGAN (Luo et al., 2022)	**No info**	**Preprocessing**: Data augmentation **Features**: FCN feature representation using Dual-decoder U-Net with suppression loss; Topological refinement GAN **Classifier**: No mention **Postprocessing**: No mention	DRIVE(20/ 40_test_ALL_PIXEL_AV) INSPIRE(40/ 40_test_ALL_CT_AV) LES-AV(11/ 22_test_ALL_PIXEL_AV)	97.00 94.20 95.10	96.80 95.20 96.10	97.20 93.20 94.10	**Advantages:** A two-stage cascaded framework that focuses on both pixel-level features and topological features of blood vessels. **Disadvantages:** The training time is lengthy, requiring more computational resources.
2020_Noh_CNN+GCN (Noh et al., 2020)	**No info**	**Preprocessing**: No mention **Features**: Parallel CNN feature representation; Hierarchical GNN feature **Classifier**: No mention **Postprocessing**: No mention	Private dataset(NP)	_	_	_	**Advantages:** Combining fundus images and FA as parallel inputs in CNN to extract features. Then using the extracted features as input for a hierarchical GNN to ensure the connectivity of blood vessels. **Disadvantages:** Data that aligns with this framework is challenging to obtain. Validation has not been performed on a publicly available dataset.
2021_Mishra_CNN+GCN (Mishra et al., 2021)	**No info**	**Preprocessing**: No mention **Features**: CNN feature representation; GCN Feature representation **Classifier**: No mention **Postprocessing**: Fusing the CNN output and the GCN output.	DRIVE(20/ 40_test_ALL_PIXEL_AV) Tongren(NP)	98.11 97.98	97.32 98.01	98.70 98.13	**Advantages:** Taking features extracted by CNN, and representing them as a graph. Inputting them into a GNN, simultaneously learning deep features and vascular topological information. **Disadvantages:** There is no corresponding post-processing method. There might be discontinuities in some blood vessels.

(*continued on next page*)

Table 4 (*continued*)

Label	Source	Method	Dataset	ACC	SE	SP	Comments
2022_GO_CNN+GNN (Go et al., 2022)	**No info**	**Preprocessing**: No mention **Features**: CNN feature representation; Dual hierarchical GNN feature **Classifier**: No mention **Postprocessing**: No mention	Private dataset(NP)	_	_	_	**Advantages:** Combining fundus images and FA as parallel inputs in CNN to extract features. Then using the extracted features as input for GNN. **Disadvantages:** Data that aligns with this method is challenging to obtain. Validation has not been performed on a publicly available dataset.
2022_Xu_CNN+GNN (Xu et al., 2023)	(xjtu-mia, xjtu-mia/octa, 2024)	**Preprocessing**: No mention **Features**: CNN feature representation; GNN Feature representation **Classifier**: No mention **Postprocessing**: No mention	Private dataset(NP)	_	_	_	**Advantages:** Using CNN to generate initial segmentation, then utilizing GNN to enhance the connectivity of the initial segmentation. **Disadvantages:** Validation has not been performed on a publicly available dataset. The cascade network has a relatively long processing time.

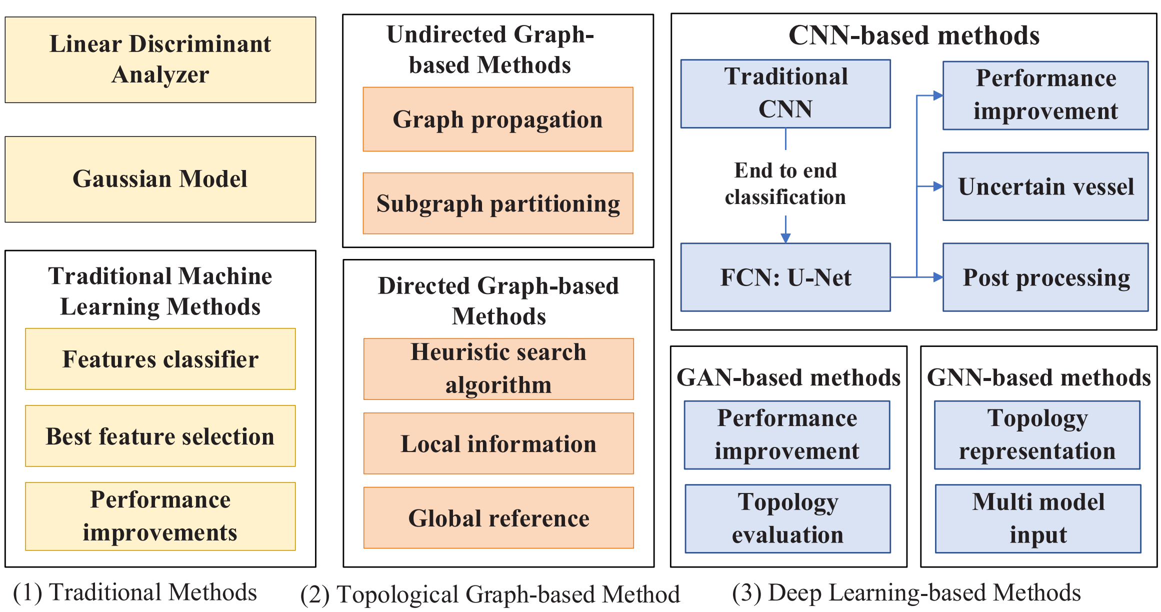

Fig. 2. Logical Framework of Automatic Classification Methods.

Mixture Model for unsupervised classification.

3.2.3. Traditional machine learning methods

Before the proposal of deep learning, traditional machine learning methods were one of the mainstream methods for arteriovenous classification.

Machine learning methods can serve as classifiers for selected features. Grisan et al (Grisan and Ruggeri, 2003). proposed a retinal arteriovenous classification method based on the ’divide et impera’ strategy. They divided the fundus image into four quadrants and then used a fuzzy clustering algorithm to cluster the arteriovenous vessels around the optic disc. Non-deep neural networks have been applied to retinal arteriovenous classification. Chhabra et al (Chhabra and Bhushan, 2014). used backpropagation networks(BPN) and probabilistic neural networks (PNN) to complete this task. Kondermann et al (Kondermann et al., 2007). used a neural network classifier and support vector machine (SVM) to classify blood vessels after principal component analysis (PCA) of vascular contour features and color features. Xu et al (Xu et al., 2017). extracted first-order and second-order image texture features of each centerline pixel and added intensity features to obtain a feature set for retinal A/V classification. They then used a KNN classifier to classify these features.

Machine learning methods can also be used to select the best feature set. Zamperini et al (Zamperini et al., 2012). focused their research on selecting the best features. They tested various feature combinations on different machine learning classifiers and ultimately demonstrated that the best features are a mixture of features related to color values and contrast around the vessels, as well as spatial information. Vijayakumar et al (Vijayakumar et al., 2016). proposed a classification method based on random forest (RF) and SVM. They used RF to select the 20 most helpful features for classification and then used these features for vessel classification using SVM. Irshad et al (Irshad et al., 2021). utilized binary particle swarm optimization to select the optimal retinal vascular features. They designed an objective function that considers the size and correlation of feature subsets when classifying retinal vessels. The designed objective function ensures that the selected feature subset contains the minimum number of features and corresponds to the maximum accuracy. After the optimization process, SVM is used to evaluate the feature subset.

Some studies have focused on exploring how to improve the performance of traditional machine learning methods with other means. Niemeijer et al (Niemeijer et al., 2009). proposed a supervised automatic method based on intensity and derivative information. They also calculated width and angle information for each vessel segment. They assigned a soft label to each pixel in the vessel segment and then determined the final result based on the pixel types of the entire vessel segment. Vázquez et al (Vázquez et al., 2010b). utilized the crease extraction algorithm to extract the vascular area near the optic disc and selected multiple sets of color features in the RGB and HSL spaces in this area. They proposed three different classification strategies based on the K-means algorithm. In subsequent research (Vázquez et al., 2010c, 2013; Saez et al., 2012), the team proposed a method based on clustering and vascular tracking. They utilized the minimum path algorithm to merge color information to improve classification performance.

There are also studies to explore the performance of machine learning Some research has also explored the performance of machine learning methods on other image modalities. Sun et al (Sun et al., 2020). considered the task of vessel classification on FA image sequences. They extracted structural features from the sequence growth information of vessels and used SVM to perform vessel classification.

3.3. Topological graph-based methods

The advantage of topological graph-based methods is their full use of topological information, but these methods require prior vascular segmentation. By extracting the skeleton of the segmented blood vessels, the corresponding topological structure is established. Finally, the arteriovenous classification of blood vessels is completed by combining topological constraints. The topology established by this method is mainly divided into undirected graphs and directed graphs.

3.3.1. Undirected graph-based methods

Undirected graph-based methods mainly achieve classification by graph propagation or subgraph partitioning, and the arteriovenous tags of edges often rely on node features and pixel color features.

Divya et al (Divya, 2015). proposed an automatic classification method for retinal arteries and veins based on graph analysis and KNN. After establishing the vascular graph structure, the labels of edges were determined using KNN based on the node type and the intensity features of the centerline pixels. This method, which only uses local features, it difficult to ensure the consistency of vascular types.

Undirected graph propagation and iteration are commonly used methods. These methods can ensure the consistency of blood vessel types. Rothaus et al (Rothaus et al., 2007, 2009). have extracted the skeleton from the pre-segmented blood vessels and established an undirected graph. Then the constraint satisfaction problem is established and the initial label is obtained by the heuristic AC3 algorithm. Finally, the problem of label conflict is solved by graph propagation. A small number of artificial tags were used during the propagation (Rothaus et al., 2007). Lin et al (Lin et al., 2009). used the extended Kalman filter to iteratively connect ungrouped segments to consider the continuity of curvature, width, and color changes at the bifurcation or crossover point.

In undirected graph-based Methods, a large part of the research is to explore how to partition the entire undirected graph into different subgraphs and then assign uniform labels to the vessels in the subgraphs. Dashtbozorg et al (Dashtbozorg et al., 2013, 2014). have determined the type of graph node (Connecting point, crossing point, meeting point, and Bifurcation point) and divided the subgraph according to the radius and angle of the undirected graph link. The graph link initial label of the subgraph is given by the node type. Then a classifier is used to complete the arteriovenous classification of the centerline pixels according to the intensity. Finally, the final classification result is obtained by combining the pixel category proportion of each graph link and the initial label. Lau et al (Lau et al., 2013). have constructed a constraint map of the vascular tree on the ROI around the optic disc and assigned vascular labels by finding the best subgraph forest. Joshi et al (Joshi et al., 2014). have used Dijkstra's shortest path algorithm to separate vascular maps. The direction, width, and strength of each vascular segment are used to find the best subgraph of the vascular segment. Finally, fuzzy C-means clustering is used to provide arteriovenous labels for each subgraph.

Hu et al (Hu et al., 2015). used a meta-heuristic algorithm to disambiguate the vascular map into different vascular trees. Firstly, the over-connected vessel potential connectivity map (VPCM) is established, and then the vascular trees are classified by morphological and intensity features, combined with the meta-learning framework. Srinidhi et al (Srinidhi et al., 2019). also used a meta-heuristic method to search the graph. The undirected graph is divided into different subtrees according to the intersection point and the bifurcation point. Then the random forest method is used to label the arteriovenous tree.

Zhao et al (Zhao et al., 2018, 2020). established the retinal vascular topology estimation and arteriovenous classification problem as a pairwise clustering problem. Using Dominant Sets Clustering, the topology estimation of the vascular tree is completed on the generated undirected graph. The vascular network is divided into different subtrees. Then the arteriovenous classification is completed according to the topological relationship combined with other features.

Pellegrini et al (Pellegrini et al., 2018). calculated the global optimal subgraph separation by graph cut approach and the linear Bayesian classifier. However, their research object is the arteriovenous classification problem of ultra-wide field of view-SLO images.

3.3.2. Directed graph-based methods

The directed graph-based methods have the advantage of incorporating direction information, which can mitigate the problems of label error propagation and subgraph error division. However, the accurate establishment of directed graphs remains a central focus and challenge of such approaches.

The inverse problem of reconstructing the vascular tree's topological structure from a planar graph is ill-posed. Moreover, the most probable tree estimation has been proven to be NP-hard (Estrada et al., 2015b). Thus, Estrada et al (Estrada et al., 2015b). used a heuristic search algorithm to obtain the optimal topology estimation of vascular trees. They proposed a general topological tree model and completed the verification of the method on the retinal dataset. The team extended the topology tree model to a topological-directed graph model (Estrada et al., 2015a). The global likelihood model is obtained by training, and the A/V label is provided by combining three features of the vascular planar graph.

The construction of directed graphs primarily relies on node-type information. The edges connected to a node are grouped based on the node type. Finally, the direction of each edge is assigned successively, starting from either the root node or the leaf nodes. De et al (De et al., 2016, 2018). proposed a novel random walk approach on directed graphs using absorbing Markov chains. They constructed a directed graph with vascular segments as nodes and the connectivity relationships between vascular segments as edges. Based on the types of vascular segment nodes, they eliminated redundant edges and defined the direction of the edges. By adjusting the label propagation on the directed graph, the vascular network graph is divided into disjoint subgraphs. This method also needs to provide additional initial labels to achieve arteriovenous classification.

Xingzheng et al. (2016). used a multi-scale curvature orientation histogram to extract vascular markers from the vascular centerline and then used local curvature direction information to modify the edge in the graph. The AV tree is tracked by the curvature direction continuity of the intersection points, and different vascular trees are separated by curvature direction clustering. This method can eliminate the problem of vascular curvature distortion in the skeletonization process.

Zhao et al. (2019). established a directed graph by combining the information of nodes and edges. Then the related parameters such as the direction and diameter information of the blood vessel are quantified. Through the constraints of relevant parameters and the parent-child edge relationship of the directed graph, they divided each edge into different subgraphs.

The optic disc can be a global reference for establishing a directed graph. The end near the optic disc is often used as the starting point of a directed edge. Martinez-Perez et al. (2020). did not build directed graphs directly. They used the optic disc as a reference to obtain vascular map direction information and identified vascular bifurcations and intersections based on direction and local geometric information. Finally, they employed fuzzy logic classification using color information for A/V classification.

3.4. Deep learning-based methods

The excellent performance and robustness of deep learning-based methods in retinal arteriovenous classification tasks make them the most prominent approach in current research. In particular, the fully convolutional network (FCN) makes it possible to directly obtain arteriovenous classification results from fundus images without prior vascular segmentation.

In this section, we will explain the logical framework of Fig. 2(3). Starting with CNN-based methods, we begin with traditional CNN methods and summarize the FCN network that can achieve end-to-end prediction. We also organize different improvements to the FCN. After that, we will discuss GAN-based and GNN-based methods, which are different improvement approaches to CNN-based methods. GAN-based methods primarily focus on improving the model's topological connectivity by improving the training framework. GNN-based methods improve the model's topological prediction ability by extracting vascular graph structure features through GNN.

3.4.1. CNN-based methods

Initially, CNN-based methods are used to classify center pixels or vascular segments, which require pre-vascular segmentation.

Welikala et al (Welikala et al., 2017). have used CNN to achieve the classification of vascular center pixels. Then the AV category of each vascular segment was determined by voting. Girard et al (Girard and Cheriet, 2017; Girard et al., 2019). have used CNN to get the initial arteriovenous score. They construct the graph according to the vascular branches and use the propagation possibility score to get the final results. The network used at this time is finally output through the fully connected layer, and such methods require pre-vascular segmentation.

U-NET has received extensive attention due to its excellent performance in medical segmentation and the advantages of end-to-end segmentation. Hemelings et al (Hemelings et al., 2019). first applied U-NET to the retinal vascular arteriovenous classification task. They completed the first arteriovenous classification without pre-vascular segmentation.

Different methods are applied to improve the classification performance of U-NET. Ma et al (Ma et al., 2019). integrated the preprocessing knowledge and vascular enhancement technology at the input end of U-NET and incorporated the Spatial Activation mechanism at the output end. Li et al (Li et al., 2020a). employed haze-removal technology for preprocessing, followed by U-Net classifying pixels into three categories: background, artery, or vein. Subsequently, a tracking algorithm was utilized to classify vascular segments. Hu et al (Hu et al., 2021). considered the constraints of vascular distribution and edge information. They incorporated vascular constraints and multi-scale features into U-Net to optimize its performance. Shin et al (Shin et al., 2020). considered topology information during the network prediction process. They transformed vascular topology estimation into iterative vascular connectivity prediction and implemented it into deep learning-based pairwise classification. The final label was determined using a voting scheme. Chowdhury et al (Chowdhury et al., 2022). introduced a self-attention module in the decoder stage to enhance the model's ability to obtain vascular structure and contextual information.

An increasing number of studies focused on the classification of uncertain blood vessels. Galdran et al (Galdran et al., 2019). completed the pixel-level uncertainty estimation by establishing a four-classification problem of arteries, veins, background, and uncertain blood vessels. Morano et al (Morano et al., 2021). have introduced a novel loss, which decomposes the joint task into three independent segmentation problems for arteries, veins, and the entire vascular network.

The difficulty of pixel-level labeling of blood vessels will lead to inconsistent labels and difficult quantification of evaluation indicators. To solve these problems, Garifullin et al (Garifullin et al., 2020). used Bayesian deep learning to analyze the prediction problem when class labels were unavailable.

Some studies have utilized post-processing techniques to refine the U-Net segmentation results. Li et al (Li et al., 2020b). have trained a concatenated network based on U-NET and post-processed it using structural information. This approach primarily addresses the prediction problems of discontinuous and label distribution deviations. Khanal et al (Khanal et al., 2022). employed U-NET to generate initial arteriovenous labels, and then utilized directed graphs and high-level operations to correct them.

3.4.2. GAN-based methods

GANs can optimize difficult-to-represent features, such as the topological structure of blood vessels, through discriminators and adversarial training. Therefore, more and more studies are using GANs for arteriovenous classification tasks.

Some studies do not directly use GAN to judge the topology but only use the adversarial training framework to improve the prediction results. Yang et al (Yang et al., 2020). used a topological structure-constrained generative adversarial network (topGAN) to complete arteriovenous classification. However, they evaluated the topological error in the study by structural similarity (SSIM) (Wei et al., 2017). Luo et al (Luo et al., 2022). have used GAN as a refinement method for initial classification. The initial AV labels are generated by U-Net with dual decoders. They used the discriminator as a feature extractor to extract features from the refined arterial/venous classification results and the ground truth. Finally, they discriminated the two features using some topology-aware loss. Some studies explore how to use the GAN framework to evaluate the topological continuity of the generated results without adding additional errors.

Chen et al (Chen et al., 2020). have used Topology Ranking GAN (TR-GAN) to improve the topological continuity of blood vessels in arteriovenous classification. They sort ground truth masks, shuffle masks, and generated masks by the discriminator. Then the continuity performance of the generator is improved through adversarial training. In subsequent studies, the team obtained Topology and Width aware GAN(TW-GAN) (Chen et al., 2022) by introducing vessel width information into TR-GAN. The width perception module predicts different width maps as auxiliary tasks to improve the performance of the main task.

Hu et al (Hu et al., 2022). first separated the predicted results of arteries and veins. Then the original image, the separated prediction results, and the ground truth are combined to obtain different combinations. By training the discriminator to identify the ground truth correspondence combination, the ability of the generative network to generate arteries and veins was improved. The study also employed additional techniques to improve the model's performance. They added a multi-scale transformation module to the encoder to achieve multi-scale information interaction across space. They also used a sample re-weighting (SW) strategy to mitigate the disturbance caused by data labeling errors.

3.4.3. GNN-based Methods

The existing methods based on the deep neural network have limitations in the expression of vascular topology information. In recent years, there have been studies using GNN to solve the above problems.

Mishra et al (Mishra et al., 2021). used graphs to represent the features extracted by CNN. Then the GCN is used to enable the model to learn the deep features of the image and the topological features of the blood vessels at the same time. The result is obtained by combining the output of CNN and GCN. Xu et al (Xu et al., 2023). studied the classification method of small arteries and veins on optical coherence tomography angiography images. They first utilized CNN to generate initial classification labels and then employed GNN to improve the connectivity of the results.

The combination of fluorescein angiography (FA) and fundus images has been explored in some studies to incorporate more information from multimodal inputs.

Noh et al (Noh et al., 2020). extracted the feature information of fundus images and FA modes through a parallel CNN. Subsequently, these features were employed as inputs to a hierarchical GNN to ensure vascular connectivity. GO et al (Go et al., 2022). also used CNN to extract features from these two image modalities. Finally, the features are input into dual hierarchical graph neural networks to achieve pixel-level classification.

4. Retinal photography and public datasets

In this section, we first introduce the common image types of fundus photography and select the most commonly used images as the research object. Next, we summarize the annotation types of different datasets. Different methods should adopt corresponding annotation types as ground truth. Finally, we organize the existing public datasets.

Most arteriovenous classification datasets are obtained by performing arteriovenous labeling on the original dataset. Therefore, this review classifies the datasets with multiple annotations according to the original datasets. The datasets with the same initial images are grouped into one class, and the labeling ideas of different datasets are sorted out. In this way, we can reflect the characteristics and development between different datasets so that later researchers can better select the dataset they need.

4.1. Retinal photography

Retinal photography refers to capturing the anatomical structure of the retina by specific devices (Zhuo et al., 2010). The main structures observed in retinal images are the optic disc, macula, blood vessels, and fovea (Fraz et al., 2012). Pathological changes in these structures are significantly associated with multiple diseases (Mookiah et al., 2013). Therefore, retinal photography plays an important role in the early diagnosis, detection, and treatment of some diseases.

Retinal images can be divided into two categories based on the acquisition equipment. One is obtained via a fundus camera equipped with a low-power microscope. The other is imaged by a laser device.

The retinal images captured by the fundus camera can be divided into color fundus images (CFI), red-free fundus images, and fluorescein angiography images. The color fundus image is obtained under white light. These images can be used to assess the health of the macular, retina, and vessels (Abdulsahib et al., 2021). In red-free imaging, the contrast between retinal vessels and other structures is improved by a red-light filter. It is used to observe vascular-related diseases such as hemorrhages and exudates (Khan et al., 2019). Fluorescein angiography (FA) images need to inject dyes into patients. Under the illumination of a specific wavelength, the fluorescence emitted by the blood vessel is photographed to obtain an image sequence. These images are mainly used for eye tumor screening and diabetic retinopathy detection (Abdulsahib et al., 2021).

The images obtained by scanning laser ophthalmoscopy (SLO) are low-exposure and directly digitally imaged (L Srinidhi et al., 2017). This method provides high-contrast images of the vascular system and can also be applied to wide-field devices (Mookiah et al., 2021).

Fig. 3 shows examples of different retinal images. This review primarily concentrates on the arteriovenous classification algorithm for color fundus images, as they remain the most commonly used in clinical settings. Laser-scanning images are also included for completeness.

4.2. Annotation types

Different types of methods need to select different annotations as ground truth. The arteriovenous annotation used by different literature can be divided into 3 categories.

1. CT (Center Line): This annotation method solely differentiates the categories of centerline pixels, lacking any vessel width information. As a result, this type of annotation is well-suited for arteriovenous classification algorithms that rely on precise vascular segmentation.
2. Pixel: This annotation method categorizes all pixels on the blood vessels into arteries and veins while retaining the width information of different blood vessels. Consequently, this annotation approach can serve as the ground truth for end-to-end methods.
3. Topo (Topology): This annotation method builds upon pixel annotation by grouping blood vessels with the same root node into coherent trees. Consequently, it can serve as the ground truth for topological graph-related methods.

Researchers perform different annotations on the same image dataset. Therefore, we categorize publicly available datasets based on the original images in the following part. A summary of the essential information and available annotation methods for each dataset category is presented.

4.3. Public datasets

4.3.1. DRIVE class

DRIVE (Digital Retinal Images for Vessel Extraction) (Staal et al., 2004) was first published for the vascular segmentation task. The dataset has a total of 40 images. 33 images were healthy fundus images and 7 images were pathological fundus images. The image size is 584×565 pixels and the field of view is 45°. The dataset is divided when given, 20 images for training and 20 images for testing.

Qureshi et al (Qureshi et al., 2013). provided an arteriovenous classification benchmark to facilitate the verification of relevant methods. They labeled and verified the DRIVE dataset to obtain pixel-level arteriovenous annotations.

Hu et al (Hu et al., 2013). also annotated the DRIVE dataset at the pixel level, publishing the dataset and naming it RITE (Retinal Images Vessel Tree Extraction).

Dashtbozorg et al (Dashtbozorg et al., 2014). have manually labeled the centerline pixels of the 20 images in the DRIVE dataset for testing. Based on (Qureshi et al., 2013), Estrada et al. (2015a) have published DRIVE's graph-structured dataset with AV labels for edges and nodes. Zhao et al. (2018) have completed the topological structure annotation

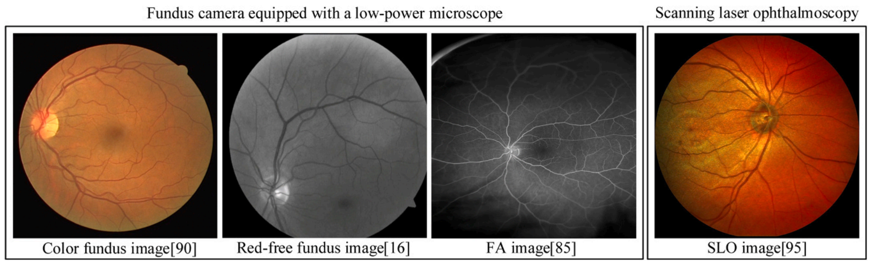

Fig. 3. Different Types of Retinal Images.

of the DRIVE dataset through two experts, and different subtrees were represented by different colors. Different types of annotations for the DRIVE dataset are shown in Fig. 4.

4.3.2. INSPIRE class

The INSPIRE-AVR dataset (Niemeijer et al., 2011) was first developed to verify the method for AVR calculation. The dataset provides 40 disc-centered fundus color images and their AVR. The image size is 2048 × 2392 pixels and the field of view is 30°.

Dashtbozorg et al (Dashtbozorg et al., 2014). have completed AV labeling of central pixels for all 40 images in INSPIRE. Estrada et al (Estrada et al., 2015a). and Zhao et al (Zhao et al., 2018). have finished the graph structure annotation and topology annotation of the dataset respectively.

4.3.3. WIDE class

The WIDE dataset was first mentioned by Estrada et al (Estrada et al., 2015b)., providing 15 high-resolution wide-field scanning laser ophthalmoscopy (SLO) images. The team supplemented WIDE in (Estrada et al., 2015a). The number of images was expanded from 15 to 30 and edge-level labeling was completed.

The dataset includes healthy eyes, as well as eyes with macular degeneration. The original image size is 3900 × 3072 pixels. After cropping and downsampling, the images become inconsistent in size. This dataset is the only known wide-field public retinal dataset.

4.3.4. HRF class

The HRF (high-resolution fundus image) dataset (Odstrcilik et al., 2013) is proposed to solve the lack of high-resolution datasets for vascular segmentation. The dataset has a total of 45 high-resolution fundus images. There were 15 healthy fundus images, 15 diabetic retinopathy images, and 15 glaucoma images. The image size is 3504 × 2336 pixels and the field of view is 60°.

To verify the algorithm, Hemelings et al (Hemelings et al., 2019). performed pixel-level AV annotation on the HRF dataset. But label the intersection area as arteries or veins.

To correct the wrong labeling of the cross area, Chen et al (Chen et al., 2022). relabeled the HRF pixel by pixel and used the color labeling different from the arteriovenous in the cross area.

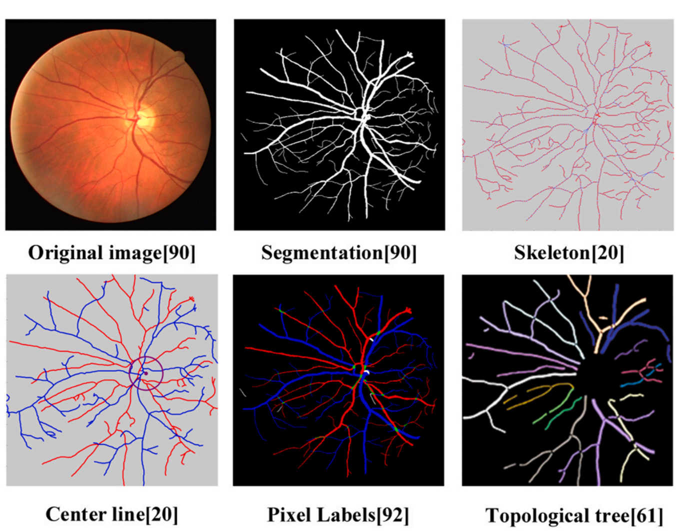

Fig. 4. Different Annotation Examples of DRIVE.

4.3.5. VICAVR class

The VICAVR dataset (Vázquez et al., 2013) was originally published to solve AVR computing tasks. The dataset currently contains 58 disc-centered retinal fundus images. The initial dataset has arteriovenous category labels and expert-labeled vascular radius. The image size is 768 × 584 pixels. Zhao et al (Zhao et al., 2018). completed the topological structure annotation of the dataset.

4.3.6. IOSTAR class

The IOSTAR dataset (Abbasi-Sureshjani et al., 2015) was first proposed to solve the problem of vascular segmentation. The dataset uses retinal images collected by SLO technology. Zhang et al (Zhang et al., 2016). expanded the dataset from 24 to 30 images and completed pixel-level arteriovenous labeling. The image size is 1024 × 1024 and the field of view is 45°. Zhao et al (Zhao et al., 2020). completed the topological structure annotation of the dataset.

4.3.7. LES-AV

The LES-AV dataset (Orlando et al., 2018) contains 22 color fundus images centered on the optic disc. The dataset provides both vascular segmentation labels and arteriovenous pixel-level classification labels. Among them, 21 images have a resolution of 1444 × 1620 pixels and a field of view of 30°. There is also a field of view of 45° FOV and a pixel of 1958 × 2196 pixels.

Table 5 records the information of each class, namely the original dataset, image type, number of images, image size and field of view, initial label, and AV ground truth.

5. Evaluation system

In this section, we refine an evaluation system for arterial-venous classification methods by incorporating insights from previous studies. This evaluation system enables a comprehensive assessment of different methods and addresses the shortcomings of topological evaluations.

First, we analyze the challenges encountered during the arterial-venous evaluation process. While the evaluation metrics may be consistent, the specific evaluation details often vary significantly. Consequently, we propose a Multi-faceted Evaluation System, drawing upon previous research, to address these challenges and provide a more comprehensive evaluation framework.

5.1. Challenges of evaluation

The evaluation of fundus vascular arteriovenous classification is more complicated than that of segmentation. For the evaluation of

Table 5
Retinal Arteriovenous Classification Public Datasets.

Original Dataset	Source	Type	Num	SIZE&FOV	Initial labels	A/V Groundtruth		
						CT	Pixel	Topo
DRIVE (Staal et al., 2004)	(DRIVE Dataset - Machine Learning Datasets,)	CFI	40	565 × 584 45°	Segmentation Labels	(Dashtbozorg et al., 2014)	(Qureshi et al., 2013; Hu et al., 2013)	(Zhao et al., 2018)
INSPIRE-AVR (Niemeijer et al., 2011)	(Inspire Datasets and Department of Ophthalmology and Visual Sciences,)	CFI	40	2392 × 2048 30∘	AVR	(Dashtbozorg et al., 2014)	_	(Zhao et al., 2018)
WIDE (Estrada et al., 2015b)	(Estrada_TMI_ and, 2015,)	SLO	30	3900 × 3072 -	_	(Estrada et al., 2015a)	_	_
HRF (Odstrcilik et al., 2013)	(High-Resolution Fundus (HRF) Image Database, n.d.)	CFI	45	3504 × 2336 -	Segmentation Labels	_	(Chen et al., 2022; Hemelings et al., 2019)	_
VICAVR (Vázquez et al., 2013)	(VARPA Group., n.d.)	CFI	58	768 × 584 -	AV Labels Radius	(Vázquez et al., 2013)	_	(Zhao et al., 2018)
IOSTAR (Abbasi-Sureshjani et al., 2015)	(IOSTAR Retinal Vessel Segmentation Dataset — bob.db. iostar 1.0.1 documentation,)	SLO	30	1024 × 1024 45°	Segmentation Labels	_	(Zhang et al., 2016)	(Zhao et al., 2020)
LES-AV (Orlando et al., 2018)	(LES-AV dataset., n.d.)	CFI	22	1444 × 1620 30° 1958 × 2196 45°	Segmentation Labels AV Labels	_	(Orlando et al., 2018)	_

segmentation, there is already a unified standard. It is established as a binary classification problem. The retinal vessels are positive samples, while the background and other tissues are negative samples. Then calculate the relevant evaluation parameters.

There is still no consistent standard for classification evaluation. Articles on retinal arteriovenous classification generally give the best results in evaluation indicators such as accuracy, sensitivity, and specificity. However, there are significant differences in vascular categories, evaluation levels, mask areas, and other evaluation details in different articles (Hemelings et al., 2019). In addition, the evaluation index of vascular continuity after classification is still insufficient.

5.1.1. Vascular category inconsistency

For the vascular categories, there are two special kinds in the ground truth besides background and arteriovenous. One is uncertain vascular type, the other is crossed vascular type. In the evaluation step, these two categories are often removed for ease of calculation and comparison (Chen et al., 2022).

For uncertain vascular pixels, the training data cannot provide accurate guidance. Galdran et al (Galdran et al., 2019). identified it as an independent type in their study. However, because the evaluation of mainstream methods is a binary classification problem. Galdran et al (Galdran et al., 2019). redistributed uncertain blood vessels between two categories of interest (arteries/veins) and calculated performance as a binary classification problem. Garifullin et al (Garifullin et al., 2020). also studied the problem of uncertainty. In the evaluation, the multi-classification problem is established into multiple binary classification problems. Vascular segmentation evaluation, arterial evaluation, and venous evaluation were performed respectively.

The crossed vascular type indicates that the blood vessel belongs to both the artery and the vein. Such pixels are of great significance for the assessment of vascular connectivity. However, in the existing evaluation methods, cross pixels are removed from the evaluation area.

5.1.2. Evaluation levels inconsistency

The evaluation level can be divided into edge level (vascular segment) and pixel level.

The edge-level evaluation method is suitable for classification algorithms based on topology graphs. This kind of method can ensure the same blood vessel category. Because this method generally has pre-vascular segmentation, there is no need to evaluate the accuracy of segmentation.

The pixel-level evaluation is divided into centerline pixels and all vascular pixels. The wide vessels can often be accurately classified and contain more pixels. Therefore, the evaluation performance of all vascular pixels is often higher than that of centerline pixels. However, the evaluation of centerline pixels cannot reflect the information on the width and vascular pixels outside the centerline. Therefore, more and more methods will be evaluated from these two perspectives.

5.1.3. Evaluation area inconsistency

The evaluation area can be divided into the whole image and the region of interest (ROI) area. The ROI region refers to the standard area from 0.5 to 1.0 times the diameter of the optic disc from the optic disc edge (Knudtson et al., 2003). The AVR is calculated through the ROI for pathological analysis and diagnosis.

Regardless of which evaluation area, a specific vascular evaluation mask should be considered. Some studies (Zhao et al., 2018, 2020; Estrada et al., 2015a; Dashtbozorg et al., 2014) calculate the relevant parameters in the region segmented by the algorithm. While some researchers (Morano et al., 2021; Chen et al., 2022, 2020) suggest that evaluation should be done in the ground truth area. When the microvessels are not segmented by the algorithm, the classification of the main retinal vessels is relatively simple. Therefore, the former is easy to get better performance. However, some pixels will always be ignored in both evaluation masks.

5.1.4. Lack of topological connectivity index

In recent years, various algorithms have begun to try to study the topological connectivity of retinal vessels. However, these methods are demonstrated through qualitative effects. Relevant quantitative evaluation indicators have yet to be developed. Shin et al (Shin et al., 2020). evaluated the continuity by quantifying the thickness and direction of vascular segments. This evaluation is performed at the edge level.

The currently known pixel-level topological connectivity metrics are infeasible (INF) and correct (COR) percentages (Chen et al., 2022; Araújo et al., 2019). These two indicators are evaluated by judging the accessibility and similarity of the selected path.

5.2. Multi-faceted evaluation system

Hemelings et al (Hemelings et al., 2019). first proposed a method combining vascular extraction and arteriovenous recognition. Therefore, they hope to specify an objective evaluation method to promote future benchmarking. Three vessel subsets (all pixels, centerline, and centerline limited to vessels wider than two pixels) are used. The evaluation of these three subsets is completed in the entire image and ROI.

However, this method has some shortcomings. On the one hand, selecting the centerlines of the retinal vessel wider two pixels will destroy the continuity of the blood vessel. This subset should not be involved in the evaluation. On the other hand, this literature did not pay attention to the pixels in the arteriovenous crossing area.

Because of the above deficiencies, we combined the work of (Chen et al., 2022; Garifullin et al., 2020; Araújo et al., 2019) to complement the above evaluation system, trying to give a more comprehensive objective benchmark evaluation system, as shown in Fig.5.

All pixels and centerline pixels are evaluated in ROI. Because ROI contains only a portion of blood vessels, connectivity cannot be evaluated. However, the accuracy of AV classification in this area is of great significance to medical diagnosis.

In the whole image, the evaluation problem is divided into vascular evaluation, arterial evaluation, and venous evaluation.

In vascular evaluation, all vascular pixels of ground truth (artery, vein, cross pixel, uncertain pixel) are unified into the vascular class, and other pixels are used as the background class. As a binary classification problem, the relevant parameters are calculated from all pixels and centerline pixels. Vascular assessment can reflect the ability of the algorithm to identify blood vessels, including uncertain blood vessels.

During artery evaluation, the artery pixels and cross pixels in the ground truth are treated as positive class and the rest as background. Also, successfully established a binary classification problem. In addition to calculating the classification of all pixels and centerline pixels in the vascular evaluation process, topological connectivity evaluation is also performed. By selecting the path, the accessibility and path accuracy of the segmented arteries are calculated.

The evaluation of the vein is the same as that of the artery. The evaluation of arteriovenous can reflect the predictive ability of the algorithm. At the same time, it also reflects the method's ability to maintain vascular topological connectivity.

6. Discussion

6.1. Quantitative analysis

We conducted a statistical analysis on 62 collected research works, hoping to solve the following problems through quantitative analysis. (1) How do the research direction and hotspots change over time, and what are the mainstream methods of current research? (2) Whether there are widely used datasets that can be employed to compare the performance of different methods? (3) What are the differences in the performance of different methods, and which methods significantly outperform other methods?.

To begin with, we generated two research heat maps by counting the number of works related to different methods across different year intervals, as demonstrated in Fig. 6 and Fig. 7. Fig. 6 reveals that topology-based graph methods were the mainstream research direction from 2013 to 2018, but since 2018, deep learning-based approaches have taken the lead.

In Fig. 7, we provide a more detailed breakdown of the methods. The main solutions before 2015 were machine learning methods and undirected graph-based approaches. After 2015 directed graph-based methods gradually received research attention. In deep learning-based research, the CNN-based method started relatively early and occupied an absolute dominant position. GAN and GNN methods have only received attention in recent years. The research heat maps allow us to conclude that while deep learning-based methods currently occupy the mainstream, topology-based methods remain an important avenue of research.

Next, we conducted a statistical analysis of the datasets used for different research evaluations. We tallied the number of times each dataset was selected by different types of research, as shown in Fig. 8. The results indicate that DRIVE and INSPIRE are commonly used datasets for evaluating all three methods. HRF and LES-AV are mainly used for deep learning-related evaluations. The frequency of dataset usage by different methods is related to the publication date and label types. Therefore, DRIVE can be used to compare the performance of different types of methods.

Furthermore, we assessed the performance of different methods on

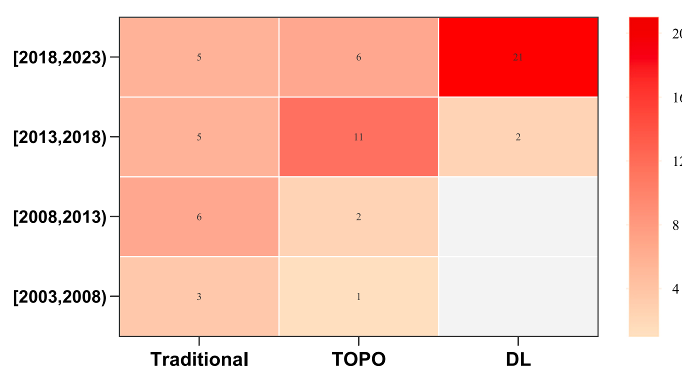

Fig. 6. Researches Distribution Heatmap1.

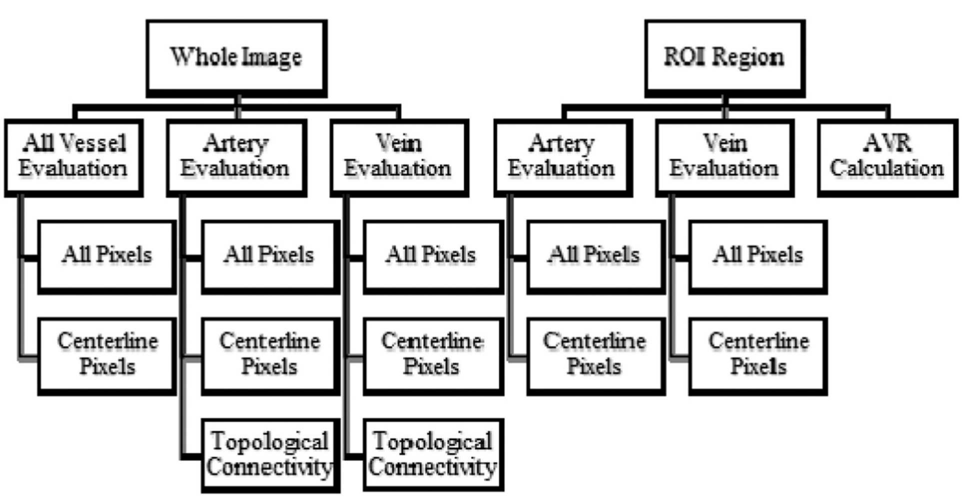

Fig. 5. Multi-faceted Evaluation System Schematic Diagram.

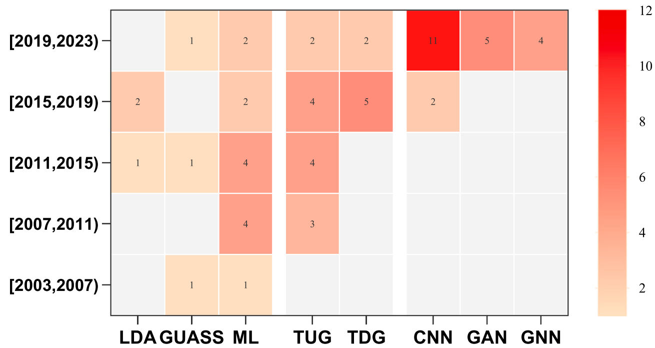

Fig. 7. Researches Distribution Heatmap 2.

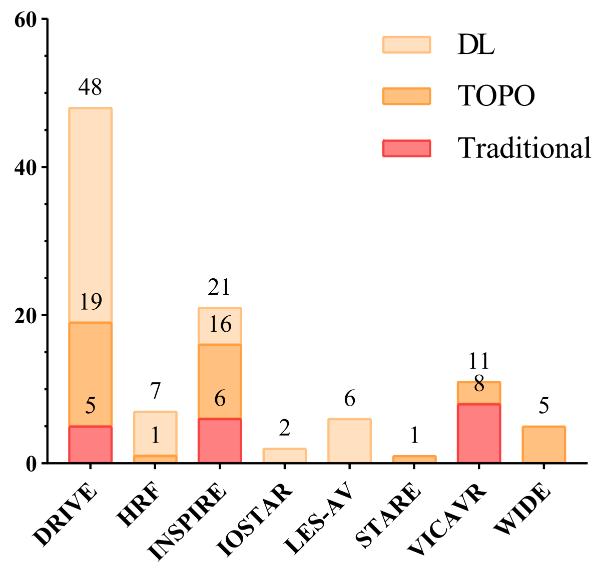

Fig. 8. Statistics of Dataset Utilization.

the DRIVE dataset. In particular, we perform independent statistics on the performance of methods combined with topological information in deep learning. The chosen evaluation metric was pixel-level accuracy. Fig. 9 illustrates the mean and extreme values of the data using box diagrams to provide a visual representation.

The methods that integrate topological information into deep learning demonstrate significantly superior performance compared to other methods. As depicted in Fig. 9, traditional methods have lost their competitiveness compared with other methods. The performance of topological graph methods is similar to that of deep learning methods. Although the deep learning methods exhibit slightly higher optimal and worst performances than the topological graph methods, their mean

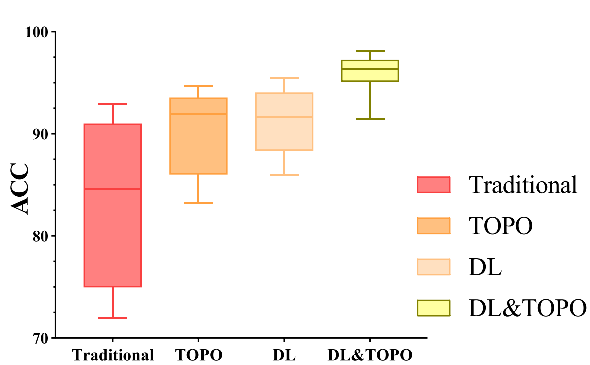

Fig. 9. The Performance of Different Methods on DRIVE.

performance is slightly lower. The methods that combine topological information with deep learning show remarkable superiority over other methods as they leverage the advantages of both approaches. We will delve into further analysis of the reasons in the next part.

6.2. *Methods comparison and future trend*

Deep learning-based methods can extract deep features of images. The fully convolutional network represented by U-NET can achieve end-to-end arteriovenous prediction. Because the topological continuity error is difficult to express, the prediction results have discontinuous blood vessels.

Therefore, most GAN-based methods are used to solve this problem. The topological expression of the generator network is optimized by training the topology discriminator.

GNN-based methods are a combination of topological graphs and deep learning. These methods can well combine the deep feature extracted by CNN with the topological structure information of blood vessels. Therefore, the classification accuracy and topological continuity are improved.

Topological graph-based methods require pre-segmentation of retinal vessels. Then graphs are constructed from the vascular skeleton. As a result, such methods depend on the segmentation results. This is an obvious deficiency of the graph-based methods.

However, these methods can make good use of the topological characteristics of retinal vessels. By judging the node type, the initial division of edges or subgraphs is realized. At the same time, the problem can be solved using graph theory, which has strong interpretability.

The directed graph-based methods ensure the consistency of the whole vascular tree through the parent-child edge relationship. However, how establishing a correct directed graph is still a problem worthy of study.

In future research, the combination of deep learning and topological graphs will become the key method to solve the problem of retinal vascular arteriovenous classification. Deep learning can be used to provide deep features for topological graphs, and the graph-based method can be used as a post-processing method for deep learning. The combination will improve the classification accuracy while maintaining the topological continuity of blood vessels.

7. Conclusion

This paper completed a comparative review of automatic retinal arteriovenous classification methods. We clarify the significance and challenges of arteriovenous classification tasks. We conduct research based on the shortcomings of the existing reviews. We organize the public datasets related to arteriovenous classification by category and development route. We also summarize the evaluation methods and propose a multi-faceted evaluation system. Finally, we summarize the advantages and disadvantages of different methods and provide a reference direction for future research. The results of the analysis show the importance of the combination of deep learning and topological information in future research.

CRediT authorship contribution statement

Liu Wanquan: Conceptualization, Supervision. **Zhao Shen:** Conceptualization, Supervision, Writing – review & editing. **Peng Jianqing:** Conceptualization, Project administration, Writing – review & editing, Supervision. **Chen Qihan:** Conceptualization, Data curation, Formal analysis, Investigation, Methodology, Writing – original draft, Writing – review & editing.

Declaration of Competing Interest

The authors declare that they have no known competing financial interests or personal relationships that could have appeared to influence the work reported in this paper.

Data availability

Data will be made available on request.

Acknowledgment

This work was supported in part by the National Key R&D Program of China under Grant 2022YFB4703103, the National Natural Science Foundation of China under Grant 62103454, and the Shenzhen Science and Technology Program under Grant JCYJ20220530150006014.

The authors would like to acknowledge Abdulsahib et al. (2021), Hu et al. (2022), Dashtbozorg et al. (2014), Zhao et al. (2018), Noh et al. (2020), Staal et al. (2004), Qureshi et al. (2013). and Abbasi-Sureshjani et al. (2015). for providing the images as open-source.

References

Abbasi-Sureshjani, S., Smit-Ockeloen, I., Zhang, J., Ter Haar Romeny, B., 2015. Biologically-inspired supervised vasculature segmentation in SLO retinal fundus images. In: Kamel, M., Campilho, A. (Eds.), Image Analysis and Recognition, vol. 9164. Springer International Publishing, Cham, pp. 325–334. https://doi.org/10.1007/978-3-319-20801-5_35.

Abdulsahib, A.A., Mahmoud, M.A., Mohammed, M.A., Rasheed, H.H., Mostafa, S.A., Maashi, M.S., 2021. Comprehensive review of retinal blood vessel segmentation and classification techniques: intelligent solutions for green computing in medical images, current challenges, open issues, and knowledge gaps in fundus medical images. Netw. Model Anal. Health Inf. Bioinforma. 10 (20) https://doi.org/10.1007/s13721-021-00294-7.

Abràmoff, M.D., Lou, Y., Erginay, A., et al., 2016. Improved automated detection of diabetic retinopathy on a publicly available dataset through integration of deep learning. Invest. Ophthalmol. Vis. Sci. 57 (13), 5200–5206. https://doi.org/10.1167/iovs.16-19964.

Alam, M.N., Le, D., Yao, X., 2021. Differential artery-vein analysis in quantitative retinal imaging: a review, 1102119–1101119, Mar Quant. Imaging Med. Surg. vol. 11 (3). https://doi.org/10.21037/qims-20-557.

Aras, R.A., Nugroho, H.A., 2020. Ardiyanto I. Measurement and classification retinal blood vessel tortuosity in digital fundus images. 2020 3rd Int. Conf. Inf. Commun. Technol. (ICOIACT) 331, 6. https://doi.org/10.1109/ICOIACT50329.2020.9332142.

Araújo, R.J., Cardoso, J.S., Oliveira, H.P., 2019. A deep learning design for improving topology coherence in blood vessel segmentation. In: Shen, D., Liu, T., Peters, T.M., Staib, L.H., Essert, C., Zhou, S., et al. (Eds.), Medical Image Computing and Computer Assisted Intervention – MICCAI 2019. Springer International Publishing, Cham, pp. 93–101. https://doi.org/10.1007/978-3-030-32239-7_11.

Araújo, T., Aresta, G., Mendonça, L., Penas, S., Maia, C., Carneiro, Â., Mendonça, A.M., Campilho, A.J., 2020. DR|GRADUATE: Uncertainty-aware deep learning-based diabetic retinopathy grading in eye fundus images. Med. Image Anal. 63, 101715.

Arnould, L., et al., . 2023. Using artificial intelligence to analyse the retinal vascular network: The future of cardiovascular risk assessment based on oculomics? A narrative review. Ophthalmol. Ther. vol. 12 (2), 657–674. https://doi.org/10.1007/s40123-022-00641-5.

Azegrouz H., Trucco E., Dhillon B., MacGillivray T., MacCormick I.J., 2006. Thickness dependent tortuosity estimation for retinal blood vessels. 2006 International Conference of the IEEE Engineering in Medicine and Biology Society; 4675:8. https://doi.org/10.1109/IEMBS.2006.260558.

Boudegga, H., Elloumi, Y., Akil, M., Hedi Bedoui, M., Kachouri, R., Abdallah, A.B., 2021. Fast and efficient retinal blood vessel segmentation method based on deep learning network. Comput. Med. Imaging Graph. 2021 90, 101902. https://doi.org/10.1016/j.compmedimag.2021.101902.

Chen, C., Chuah, J.H., Ali, R., Wang, Y., 2021. Retinal vessel segmentation using deep learning: a review. IEEE Access 9, 111985–112004. https://doi.org/10.1109/ACCESS.2021.3102176.

Chen, W., Yu, S., Wu, J., Ma, K., Bian, C., Chu, C., et al., 2020. TR-GAN: Topology ranking GAN with triplet loss for retinal artery/vein classification. In: Martel, A.L., Abolmaesumi, P., Stoyanov, D., Mateus, D., Zuluaga, M.A., Zhou, S.K., et al. (Eds.), Medical Image Computing and Computer Assisted Intervention – MICCAI 2020. Springer International Publishing, Cham, pp. 616–625. https://doi.org/10.1007/978-3-030-59722-1_59.

Chen, W., Yu, S., Ma, K., Ji, W., Bian, C., Chu, C., et al., 2022. TW-GAN: Topology and width aware GAN for retinal artery/vein classification. Med. Image Anal. 77, 102340 https://doi.org/10.1016/j.media.2021.102340.

Cheung, C.S., Butty, Z., Tehrani, N.N., Lam, W.C., 2011b. Computer-assisted image analysis of temporal retinal vessel width and tortuosity in retinopathy of prematurity for the assessment of disease severity and treatment outcome. J. Am. Assoc. Pediatr. Ophthalmol. Strabismus 15 (4), 374–380.

Cheung, C.S.Y., Butty, Z., Tehrani, N.N., Lam, W.C., 2011a. Computer-assisted image analysis of temporal retinal vessel width and tortuosity in retinopathy of prematurity for the assessment of disease severity and treatment outcome. J. Am. Assoc. Pediatr. Ophthalmol. Strabismus 15, 374–380. https://doi.org/10.1016/j.jaapos.2011.05.008.

Chew, S.K.H., Xie, J., Wang, J.J., 2012a. Retinal arteriolar diameter and the prevalence and incidence of hypertension: a systematic review and meta-analysis of their association. Curr. Hypertens. Rep. 14, 144–151. https://doi.org/10.1007/s11906-012-0252-0.

Chew, S.K.H., Xie, J., Wang, J.J., 2012b. Retinal arteriolar diameter and the prevalence and incidence of hypertension: a systematic review and meta-analysis of their association. Curr. Hypertens. Rep. 14, 144–151. https://doi.org/10.1007/s11906-012-0252-0.

Chhabra, S., Bhushan, B., 2014. Supervised pixel classification into arteries and veins of retinal images. 2014 innovative applications of computational intelligence on power. Energy Controls their Impact Humanit. (CIPECH) 59–62. https://doi.org/10.1109/CIPECH.2014.7019098.

Chowdhury, A.Z.M.E., Mann, G., Morgan, W.H., Vukmirovic, A., Mehnert, A., Sohel, F., 2022. MSGANet-RAV: A multiscale guided attention network for artery-vein segmentation and classification from optic disc and retinal images. J. Optom. 15, S58–S69. https://doi.org/10.1016/j.optom.2022.11.001.

da Silva, A.V.B., Gouvea, S.A., da Silva, A.P.B., Bortolon, S., Rodrigues, A.N., Abreu, G.R., et al., 2015. Changes in retinal microvascular diameter in patients with diabetes. Int J. Gen. Med 8, 267–273. https://doi.org/10.2147/IJGM.S83749.

Daich Varela, M., Sen, S., De Guimaraes, T.A.C., et al., 2023. Artificial intelligence in retinal disease: clinical application, challenges, and future directions. Graefes Arch. Clin. Exp. Ophthalmol. 261, 3283–3297. https://doi.org/10.1007/s00417-023-06052-x.

Dashtbozorg, B., Mendonça, A.M., Campilho, A., 2013. Automatic estimation of the arteriolar-to-venular ratio in retinal images using a graph-based approach for artery/vein classification. In: Kamel, M., Campilho, A. (Eds.), Image Analysis and Recognition. Springer, Berlin, Heidelberg, pp. 530–538. https://doi.org/10.1007/978-3-642-39094-4_60.

Dashtbozorg, B., Mendonca, A.M., Campilho, A., 2014. An automatic graph-based approach for artery/vein classification in retinal images. IEEE Trans. Image Process 23, 1073–1083. https://doi.org/10.1109/TIP.2013.2263809.

De, J., Cheng, L., Zhang, X., Lin, F., Li, H., Ong, K.H., et al., 2016. A graph-theoretical approach for tracing filamentary structures in neuronal and retinal images. IEEE Trans. Med Imaging 35, 257–272. https://doi.org/10.1109/TMI.2015.2465962.

De, J., Zhang, X., Lin, F., Cheng, L., 2018. Transduction on directed graphs via absorbing random walks. IEEE Trans. Pattern Anal. Mach. Intell. 40, 1770–1784. https://doi.org/10.1109/TPAMI.2017.2730871.

Divya, M., 2015. Vessels classification in retinal images by graphbased approach (Auricle Technologies Pvt. Ltd). IJRITCC 3, 1646–1648. https://doi.org/10.17762/ijritcc2321-8169.1503163.

DRIVE Dataset - Machine Learning Datasets, (n.d.). ⟨https://datasets.activeloop.ai/docs/ml/datasets/drive-dataset/⟩ (accessed February 1, 2024).

Estrada, R., Allingham, M.J., Mettu, P.S., Cousins, S.W., Tomasi, C., Farsiu, S., 2015a. Retinal artery-vein classification via topology estimation. IEEE Trans. Med Imaging 34, 2518–2534. https://doi.org/10.1109/TMI.2015.2443117.

Estrada, R., Tomasi, C., Schmidler, S.C., Farsiu, S., 2015b. Tree topology estimation. IEEE Trans. Pattern Anal. Mach. Intell. 37, 1688–1701. https://doi.org/10.1109/TPAMI.2014.2382116.

Estrada_TMI_. 2015, (n.d.). https://people.duke.edu/~sf59/Estrada_TMI_ 2015_dataset.htm (accessed February 1, 2024).

Fraz, M.M., Remagnino, P., Hoppe, A., Uyyanonvara, B., Rudnicka, A.R., Owen, C.G., et al., 2012. Blood vessel segmentation methodologies in retinal images–a survey. Comput. Methods Prog. Biomed. 108, 407–433. https://doi.org/10.1016/j.cmpb.2012.03.009.

Galdran, A., Meyer, M., Costa, P., MendonÇa, Campilho, A., 2019. Uncertainty-aware artery/vein classification on retinal images. 2019 IEEE 16th Int. Symp. . Biomed. Imaging (ISBI 2019) 556–560. https://doi.org/10.1109/ISBI.2019.8759380.

Garifullin, A., Lensu, L., Uusitalo, H., 2020. On the uncertainty of retinal artery-vein classification with dense fully-convolutional neural networks. In: Blanc-Talon, J., Delmas, P., Philips, W., Popescu, D., Scheunders, P. (Eds.), Advanced Concepts for Intelligent Vision Systems, vol. 12002. Springer International Publishing, Cham, pp. 87–98. https://doi.org/10.1007/978-3-030-40605-9_8.

Girard, F., Cheriet, F., 2017. Artery/vein classification in fundus images using CNN and likelihood score propagation. 2017 IEEE Glob. Conf. Signal Inf. Process. (Glob.) 720–724. https://doi.org/10.1109/GlobalSIP.2017.8309054.

Girard, F., Kavalec, C., Cheriet, F., 2019. Joint segmentation and classification of retinal arteries/veins from fundus images. Artif. Intell. Med. 94, 96–109. https://doi.org/10.1016/j.artmed.2019.02.004.

GitHub - agaldran/a_v_uncertain: Code for our ISBI 2019 paper on Artery/Vein classification with uncertainty predictions, (n.d.). ⟨https://github.com/agaldran/a_v_uncertain⟩ (accessed February 1, 2024).

GitHub - conscienceli/SeqNet: Joint Learning of Vessel Segmentation and Artery/Vein Classification, (n.d.). https://github.com/conscienceli/ SeqNet (Accessed February 1, 2024).

GitHub - o0t1ng0o/TW-GAN: This is the pytorch implementation for TW-GAN., (n.d.). https://github.com/o0t1ng0o/TW-GAN (Accessed February 1, 2024).

GitHub - rubenhx/av-segmentation, (n.d.). https://github.com/rubenhx /av-segmentation (Accessed February 1, 2024).

Go, S., Kim, J., Noh, K.J., Park, S.J., Lee, S., 2022. Combined deep learning of fundus images and fluorescein angiography for retinal artery/vein classification. IEEE Access 10, 70688–70698. https://doi.org/10.1109/ACCESS.2022.3187503.

Grisan, E., Ruggeri, A., 2003. A divide et impera strategy for automatic classification of retinal vessels into arteries and veins. Vol.1 Proc. 25th Annu. Int. Conf. IEEE Eng.

Med. Biol. Soc. (IEEE Cat. No. 03CH37439) vol. 1, 890–893. https://doi.org/10.1109/IEMBS.2003.1279908.

Guan, K., Hudson, C., Wong, T., Kisilevsky, M., Nrusimhadevara, R.K., Lam, W.C., et al., 2006a. Retinal hemodynamics in early diabetic macular edema. Diabetes 55, 813–818. https://doi.org/10.2337/diabetes.55.03.06.db05-0937.

Guan, Hudson, K., Wong, C., Kisilevsky, T., Nrusimhadevara, M., Lam, R.K., Mandelcorn, W.C., Devenyi, M., J.G, R.G.Flanagan, 2006b. Retinal hemodynamics in early diabetic macular edema. Diabetes 55 (3), 813–818.

Hemelings, R., Elen, B., Stalmans, I., Van Keer, K., De Boever, P., Blaschko, M.B., 2019. Artery–vein segmentation in fundus images using a fully convolutional network. Comput. Med. Imaging Graph. 76, 101636 https://doi.org/10.1016/j.compmedimag.2019.05.004.

High-Resolution Fundus (HRF) Image Database, (n.d.). ⟨https://www5.cs.fau.de/research/data/fundus-images/⟩ (Accessed February 1, 2024).

Homepage of Yitian Zhao, (n.d.). ⟨https://ytianzhao.github.io/⟩ #Code-pages (Accessed February 1, 2024).

Hu, J., Wang, H., Cao, Z., Wu, G., Jonas, J.B., Wang, Y.X., et al., 2021. Automatic artery/vein classification using a vessel-constraint network for multicenter fundus images. Front Cell Dev. Biol. 9, 659941 https://doi.org/10.3389/fcell.2021.659941.

Hu, J., Wang, H., Wu, G., Cao, Z., Mou, L., Zhao, Y., et al., 2022. Multi-scale interactive network with artery/vein discriminator for retinal vessel classification. In: IEEE Journal of Biomedical and Health Informatics, 26, pp. 3896–3905. https://doi.org/10.1109/JBHI.2022.3165867.

Hu, Q., Abràmoff, M.D., Garvin, M.K., 2013. Automated separation of binary overlapping trees in low-contrast color retinal images. Med Image Comput. Comput. Assist Inter. 16, 436–443. https://doi.org/10.1007/978-3-642-40763-5_54.

Hu, Q., Abràmoff, M.D., Garvin, M.K., 2015. Automated construction of arterial and venous trees in retinal images. J. Med Imaging (Bellingham 2, 044001. https://doi.org/10.1117/1.JMI.2.4.044001.

Huang, F., Dashtbozorg, B., ter Haar Romeny, B., 2018a. Artery/vein classification using reflection features in retina fundus images. Mach. Vis. Appl. 29 https://doi.org/10.1007/s00138-017-0867-x.

Huang, F., Dashtbozorg, B., Tan, T., ter Haar Romeny, B.M., 2018b. Retinal artery/vein classification using genetic-search feature selection. Comput. Methods Prog. Biomed. 161, 197–207. https://doi.org/10.1016/j.cmpb.2018.04.016.

Inspire Datasets | Department of Ophthalmology and Visual Sciences, (n.d.). ⟨https://medicine.uiowa.edu/eye/inspire-datasets⟩ (Accessed February 1, 2024).

IOSTAR Retinal Vessel Segmentation Dataset — bob.db.iostar 1.0.1 documentation, (n.d.). ⟨https://www.idiap.ch/software/bob/docs/bob/bob⟩. db. iostar/stable/ (Accessed February 1, 2024).

Iqbal, S., Khan, T.M., Naveed, K., Naqvi, S.S., Nawaz, S.J., 2022. Recent trends and advances in fundus image analysis: a review. Comput. Biol. Med. 151, 106277 https://doi.org/10.1016/j.compbiomed.2022, 106277.S.

Irshad, S., Yin, X., Zhang, Y., 2021. A new approach for retinal vessel differentiation using binary particle swarm optimization. Comput. Methods Biomech. Biomed. Eng. Imaging Vis. 9, 510–522. https://doi.org/10.1080/21681163.2020.1870001.

Jia, D., Zhuang, X., 2021. Learning-based algorithms for vessel tracking: a review. Comput. Med. Imaging Graph. 2020 89, 101840. https://doi.org/10.1016/j.compmedimag.2020.101840.

Joshi, V.S., Reinhardt, J.M., Garvin, M.K., Abramoff, M.D., 2014. Automated method for identification and artery-venous classification of vessel trees in retinal vessel networks. PLoS One 9, e88061. https://doi.org/10.1371/journal.pone.0088061.

Khan, K.B., Khaliq, A.A., Jalil, A., Iftikhar, M.A., Ullah, N., Aziz, M.W., et al., 2019. A review of retinal blood vessels extraction techniques: challenges, taxonomy, and future trends. Pattern Anal. Applic 22, 767–802. https://doi.org/10.1007/s10044-018-0754-8.

Khanal A., Motevali S., Estrada R. Fully Automated Tree Topology Estimation and Artery-Vein Classification 2022. https://doi.org/10.48550/arXiv.2202.02382.

Knudtson, M.D., Lee, K.E., Hubbard, L.D., Wong, T.Y., Klein, R., Klein, B.E.K., 2003. Revised formulas for summarizing retinal vessel diameters. Curr. Eye Res. 27, 143–149. https://doi.org/10.1076/ceyr.27.3.143.16049.

Kondermann, C., Kondermann, D., Yan, M., 2007. In: Pluim, J.P.W., Reinhardt, J.M. (Eds.), Blood vessel classification into arteries and veins in retinal images. San Diego, CA. https://doi.org/10.1117/12.708469.

L Srinidhi, C., Aparna, P., Rajan, J., 2017. Recent advancements in retinal vessel segmentation. J. Med Syst. 41, 70. https://doi.org/10.1007/s10916-017-0719-2.

Lau, Q.P., Mong Li Lee, Hsu, W., Wong, Tien Yin, 2013. Simultaneously identifying all true vessels from segmented retinal images. IEEE Trans. Biomed. Eng. 60, 1851–1858. https://doi.org/10.1109/TBME.2013.2243447.

LES-AV dataset, (n.d.). ⟨https://figshare.com/articles/dataset/LES-AV⟩ _dataset/11857698 (Accessed February 1, 2024).

Li, H., Hsu, W., Lee, M.L., Wang, H., 2003. A piecewise Gaussian model for profiling and differentiating retinal vessels. Proc. 2003 Int. Conf. Image Process. (Cat. No. 03CH37429) vol. 1, I–1069. https://doi.org/10.1109/ICIP.2003.1247151.

Li L., Verma M., Nakashima Y., Kawasaki R., Nagahara H. Joint Learning of Vessel Segmentation and Artery/Vein Classification with Post-processing 2020b. https://doi.org/10.48550/arXiv.2005.13337.

Li, P., Deng, Q., Li, H., 2020a. The arteriovenous classification in retinal images by U-net and tracking algorithm. 2020 IEEE 5th Int. Conf. Image, Vis. Comput. (ICIVC) 182–187. https://doi.org/10.1109/ICIVC50857.2020.9177446.

Lin, K.-S., Tsai, C.-L., Sofka, M., Tsai, C.-H., Chen, S.-J., Lin, W.-Y., 2009. Vascular tree construction with anatomical realism for retinal images. 2009 Ninth IEEE International Conference on Bioinformatics and BioEngineering, Taichung. IEEE, Taiwan, pp. 313–318. https://doi.org/10.1109/BIBE.2009.18.

Luo, S., Heng, Z., Pagnucco, M., Song, Y., 2022. Two-stage topological refinement network for retinal artery/vein classification. 2022 IEEE 19th Int. Symp. Biomed. Imaging (ISBI) 1–4. https://doi.org/10.1109/ISBI52829.2022.9761669.

Ma, W., Yu, S., Ma, K., Wang, J., Ding, X., Zheng, Y., 2019. Multi-task neural networks with spatial activation for retinal vessel segmentation and artery/vein classification. In: Shen, D., Liu, T., Peters, T.M., Staib, L.H., Essert, C., Zhou, S., et al. (Eds.), Medical Image Computing and Computer Assisted Intervention – MICCAI 2019, vol. 11764. Springer International Publishing, Cham, pp. 769–778. https://doi.org/10.1007/978-3-030-32239-7_85.

Martinez-Perez, M.E., Parker, K.H., Witt, N., Hughes, A.D., Thom, S.A., 2020. Automatic artery/vein classification in colour retinal images. In: Osten, W., Nikolaev, D.P. (Eds.), Twelfth International Conference on Machine Vision (ICMV 2019). SPIE, Amsterdam, Netherlands, p. 52. https://doi.org/10.1117/12.2557519.

Miri, M., Amini, Z., Rabbani, H., Kafieh, R., 2017. A comprehensive study of retinal vessel classification methods in fundus images. J. Med Signals Sens 7, 59–70.

Mirsharif, Q., Tajeripour, F., Pourreza, H., 2013. Automated characterization of blood vessels as arteries and veins in retinal images. Comput. Med Imaging Graph 37, 607–617. https://doi.org/10.1016/j.compmedimag.2013.06.003.

Mishra, S., Wang, Y.X., Wei, C.C., Chen, D.Z., Hu, X.S., 2021. VTG-Net: A CNN based vessel topology graph network for retinal artery/vein classification. Front. Med. 8, 750396 https://doi.org/10.3389/fmed.2021.750396.

Mookiah, M.R.K., Acharya, U.R., Chua, C.K., Lim, C.M., Ng, E.Y.K., Laude, A., 2013. Computer-aided diagnosis of diabetic retinopathy: a review. Comput. Biol. Med. 43, 2136–2155. https://doi.org/10.1016/j.compbiomed.2013.10.007.

Mookiah, M.R.K., Hogg, S., MacGillivray, T.J., Prathiba, V., Pradeepa, R., Mohan, V., et al., 2021. A review of machine learning methods for retinal blood vessel segmentation and artery/vein classification. Med. Image Anal. 68, 101905 https://doi.org/10.1016/j.media.2020.101905.

Morano, J., Hervella, Á.S., Novo, J., Rouco, J., 2021. Simultaneous segmentation and classification of the retinal arteries and veins from color fundus images. Artif. Intell. Med. 118, 102116 https://doi.org/10.1016/j.artmed.2021.102116.

Niemeijer, M., Staal, J., van Ginneken, B., Loog, M., Abramoff, M.D., 2004. In: Fitzpatrick, J.M., Sonka, M. (Eds.), Comparative study of retinal vessel segmentation methods on a new publicly available database. San Diego, CA, p. 648. https://doi.org/10.1117/12.535349.

Niemeijer M., van Ginneken B., Abràmoff M.D. Automatic classification of retinal vessels into arteries and veins. In: Karssemeijer N, Giger ml, editors., Lake Buena Vista, FL: 2009, p. 72601F. https://doi.org/10.1117/12.813826.

Niemeijer, M., Xiayu, Xu, Dumitrescu, A.V., Gupta, P., van Ginneken, B., Folk, J.C., et al., 2011. Automated measurement of the arteriolar-to-venular width ratio in digital color fundus photographs. IEEE Trans. Med Imaging 30, 1941–1950. https://doi.org/10.1109/TMI.2011.2159619.

Noh, K.J., Park, S.J., Lee, S., 2020. Combining fundus images and fluorescein angiography for artery/vein classification using the hierarchical vessel graph network. In: Martel, A.L., Abolmaesumi, P., Stoyanov, D., Mateus, D., Zuluaga, M.A., Zhou, S.K., et al. (Eds.), Medical Image Computing and Computer Assisted Intervention – MICCAI 2020. Springer International Publishing, Cham, pp. 595–605. https://doi.org/10.1007/978-3-030-59722-1_57.

Odstrcilik, J., Kolar, R., Budai, A., Hornegger, J., Jan, J., Gazarek, J., et al., 2013. Retinal vessel segmentation by improved matched filtering: evaluation on a new high-resolution fundus image database. IET Image Process. 7, 373–383. https://doi.org/10.1049/iet-ipr.2012.0455.

Orlando, J.I., Barbosa Breda, J., van Keer, K., Blaschko, M.B., Blanco, P.J., Bulant, C.A., 2018. Towards a glaucoma risk index based on simulated hemodynamics from fundus images. In: Frangi, A.F., Schnabel, J.A., Davatzikos, C., Alberola-López, C., Fichtinger, G. (Eds.), Medical Image Computing and Computer Assisted Intervention – MICCAI 2018. Springer International Publishing, Cham, pp. 65–73. https://doi.org/10.1007/978-3-030-00934-2_8.

Pellegrini, E., Robertson, G., MacGillivray, T., van Hemert, J., Houston, G., Trucco, E., 2018. A graph cut approach to artery/vein classification in ultra-widefield scanning laser ophthalmoscopy. IEEE Trans. Med. Imaging 37, 516–526. https://doi.org/10.1109/TMI.2017.2762963.

Qureshi, T.A., Habib, M., Hunter, A., Al-Diri, B., 2013. A manually-labeled, artery/vein classified benchmark for the DRIVE dataset. Proc. 26th IEEE Int. Symp. . Comput. -Based Med. Syst. 485–488. https://doi.org/10.1109/CBMS.2013.6627847.

Rajalakshmi, R., Subashini, R., Anjana, R.M., et al., 2018. Automated diabetic retinopathy detection in smartphone-based fundus photography using artificial intelligence. Eye 32, 1138–1144. https://doi.org/10.1038/s41433-018-0064-9.

Relan, D., Relan, R., 2021. Unsupervised sorting of retinal vessels using locally consistent Gaussian mixtures. Comput. Methods Prog. Biomed. 199 (105894) https://doi.org/10.1016/j.cmpb.2020.105894.

Relan, D., MacGillivray, T., Ballerini, L., Trucco, E., 2013. Retinal vessel classification: sorting arteries and veins. Annu Int Conf. IEEE Eng. Med Biol. Soc. 2013, 7396–7399. https://doi.org/10.1109/EMBC.2013.6611267.

Ribeiro, L., Oliveira C, M., Neves, C., Ramos J, D., Ferreira, H., Cunha-Vaz, J., 2015. Screening for diabetic retinopathy in the central region of Portugal. Added value of automated 'disease/no disease' grading. Ophthalmologica 1 233 (2), 96–103. https://doi.org/10.1159/000368426.

Rothaus, K., Rhiem, P., Jiang, X., 2007. Separation of the retinal vascular graph in arteries and veins. Proceedings of the 6th IAPR-TC-15 international conference on Graph-based representations in pattern recognition. Springer-Verlag, Berlin, Heidelberg, pp. 251–262.

Rothaus, K., Jiang, X., Rhiem, P., 2009. Separation of the retinal vascular graph in arteries and veins based upon structural knowledge. Image Vis. Comput. 27 (864–75), 013. https://doi.org/10.1016/j.imavis.2008.02.

Saez, M., González-Vázquez, S., González-Penedo, M., Barceló, M.A., Pena-Seijo, M., Coll de Tuero, G., et al., 2012. Development of an automated system to classify retinal vessels into arteries and veins. Comput. Methods Prog. Biomed. 108, 367–376.

Salamat, N., Missen, M.M.S., Rashid, A., 2019. Diabetic retinopathy techniques in retinal images: a review. Artif. Intell. Med. 97, 168–188. https://doi.org/10.1016/j.artmed.2018.10.009.

Shin, S.Y., Lee, S., Yun, I.D., Lee, K.M., 2020. Topology-aware retinal artery–vein classification via deep vascular connectivity prediction. Appl. Sci. 11, 320. https://doi.org/10.3390/app11010320.

Singh, S., Tiwari, R.K., 2019. A review on retinal vessel segmentation and classification methods. 2019 3rd Int. Conf. Trends Electron. Inform. (ICOEI) 895–900. https://doi.org/10.1109/ICOEI.2019.8862555.

Smith W., Wang J.J., Wong T.Y., Rochtchina E., Klein R., Leeder S.R., Mitchell P. Retinal arteriolar narrowing is associated with 5-year incident severe hypertension: The Blue Mountains Eye Study,(2004) Hypertension, 44 (4), pp. 442 - 447 DOI: 10.1161/01.HYP.0000140772.40322.ec.

Soomro, T.A., Afifi, A.J., Zheng, L., Soomro, S., Gao, J., Hellwich, O., et al., 2019. Deep learning models for retinal blood vessels segmentation: a review. IEEE Access 7, 71696–71717. https://doi.org/10.1109/ACCESS.2019.2920616.

Srinidhi, C.L., Aparna, P., Rajan, J., 2019. Automated method for retinal artery/vein separation via graph search metaheuristic approach. IEEE Trans. Image Process. 28, 2705–2718. https://doi.org/10.1109/TIP.2018.2889534.

Staal, J., Abramoff, M.D., Niemeijer, M., Viergever, M.A., van Ginneken, B., 2004. Ridge-based vessel segmentation in color images of the retina. IEEE Trans. Med. Imaging 23 (501–9). https://doi.org/10.1109/TMI.2004.825627.

Sule, O.O., 2022. A survey of deep learning for retinal blood vessel segmentation methods: taxonomy, trends, challenges and future directions. IEEE Access 10, 38202–38236. https://doi.org/10.1109/ACCESS.2022.3163247.

Sun, G., Liu, X., Gong, J., Gao, L., 2020. Artery-venous classification in fluorescein angiograms based on region growing with sequential and structural features. Comput. Methods Prog. Biomed. 190, 105340 https://doi.org/10.1016/j.cmpb.2020.105340.

Sutter, F.K.P., Helbig, H., 2003. Familial Retinal Arteriolar Tortuosity: A Review. Surv. Ophthalmol. 48, 245–255. https://doi.org/10.1016/S0039-6257(03)00029-8.

syshin1014, syshin1014/VCP, 2020. https://github.com/syshin1014/ VCP (Accessed February 1, 2024).

Tramontan, L., Grisan, E., Ruggeri, A., 2008. An improved system for the automatic estimation of the Arteriolar-to-Venular diameter Ratio (AVR) in retinal images. 2008 30th Annu. Int. Conf. IEEE Eng. Med. Biol. Soc. 3550–3553. https://doi.org/10.1109/IEMBS.2008.4649972.

TwistedW, TwistedW/MIAV, 2023. https://github.com/TwistedW/MI AV (Accessed February 1, 2024).

VARPA Group, (n.d.). ⟨http://www.varpa.es/research/ophtalmology.html⟩ (Accessed February 1, 2024).

Vázquez, S.G., Barreira, N., Penedo, M.G., Saez, M., Pose-Reino, A., 2010a. Using retinex image enhancement to improve the artery/vein classification in retinal images. In: Campilho, A., Kamel, M. (Eds.), Image Analysis and Recognition, 6112, pp. 50–59. https://doi.org/10.1007/978-3-642-13775-4_6.

Vázquez, S.G., Barreira, N., Penedo, M.G., Ortega, M., Pose-Reino, A., 2010b. Improvements in retinal vessel clustering techniques: towards the automatic computation of the arteriovenous ratio. Computing 90, 197–217. https://doi.org/10.1007/s00607-010-0114-z.

Vázquez, S.G., Cancela, B., Barreira, N., Penedo, M.G., Saez, M., 2010c. On the automatic computation of the arterio-venous ratio in retinal images: using minimal paths for the artery/vein classification. 2010 Int. Conf. Digit. Image Comput.: Tech. Appl. 599–604. https://doi.org/10.1109/DICTA.2010.106.

Vázquez, S.G., Cancela, B., Barreira, N., Penedo, M.G., Rodríguez-Blanco, M., Pena Seijo, M., et al., 2013. Improving retinal artery and vein classification by means of a minimal path approach. Mach. Vis. Appl. 24, 919–930. https://doi.org/10.1007/s00138-012-0442-4.

Vijayakumar, V., Koozekanani, D.D., White, R., Kohler, J., Roychowdhury, S., Parhi, K. K., 2016. Artery/vein classification of retinal blood vessels using feature selection. Annu Int Conf. IEEE Eng. Med Biol. Soc. 2016, 1320–1323. https://doi.org/10.1109/EMBC.2016.7590950.

Wei, Y., Wang, Z., Xu, M., 2017. Road structure refined CNN for road extraction in aerial image. IEEE Geosci. Remote Sens. Lett. 14, 709–713. https://doi.org/10.1109/LGRS.2017.2672734.

Welikala, R.A., Foster, P.J., Whincup, P.H., Rudnicka, A.R., Owen, C.G., Strachan, D.P., et al., 2017. Automated arteriole and venule classification using deep learning for retinal images from the UK Biobank cohort. Comput. Biol. Med 90, 23–32. https://doi.org/10.1016/j.compbiomed.2017.09.005.

Wong, Klein, T.Y., Klein, R., Tielsch, B.E., Hubbard, J.M., F.J, L.Nieto, 2001. Retinal microvascular abnormalities and their relationship with hypertension, cardiovascular disease, and mortality. Surv. Ophthalmol. 46 (1), 59–80.

Wong, T.Y., Klein, R., Sharrett, A.R., et al., 2002. Retinal arteriolar narrowing and risk of coronary heart disease in men and women: the atherosclerosis risk in communities study. JAMA 287 (9), 1153–1159. https://doi.org/10.1001/jama.287.9.1153.

Wong, Klein, T.Y., Sharrett, R., Manolio, A.R., Hubbard, T.A., Marino, L.D., Kuller, E.K., Burke, L., Tracy, G., R.P. Polak, J.F., et al., 2003. The prevalence and risk factors of retinal microvascular abnormalities in older persons: the cardiovascular health study. Ophthalmology 110 (4), 658–666.

Xingzheng, Lyu, Qifan, Yang, Shunren, Xia, Sanyuan, Zhang, 2016. Construction of retinal vascular trees via curvature orientation prior. 2016 IEEE International Conference on Bioinformatics and Biomedicine (BIBM), Shenzhen. IEEE,, China, pp. 375–382. https://doi.org/10.1109/BIBM.2016.7822548.

xjtu-mia, xjtu-mia/octa, 2024. https://github.com/xjtu-mia/octa (Accessed February 1, 2024).

Xu, X., Ding, W., Abràmoff, M.D., Cao, R., 2017. An improved arteriovenous classification method for the early diagnostics of various diseases in retinal image. In: Comput Methods Programs Biomed, 141, pp. 3–9. https://doi.org/10.1016/j.cmpb.2017.01.007.

Xu, X., Yang, P., Wang, H., Xiao, Z., Xing, G., Zhang, X., et al., 2023. AV-casNet: Fully automatic arteriole-venule segmentation and differentiation in OCT angiography. IEEE Trans. Med. Imaging 42, 481–492. https://doi.org/10.1109/TMI.2022.3214291.

Yan, Y., You, Z., Huang, W., 2021. A Review of the classification of artery and vein retinal vessels based on machine learning. 2021 IEEE Intl Conf on Dependable, Autonomic and Secure Computing, Intl Conf on Pervasive Intelligence and Computing, Intl Conf on Cloud and Big Data Computing. Intl Conf on Cyber Science and Technology Congress (DASC/PiCom/CBDCom/CyberSciTech), AB. IEEE, Canada, pp. 767–774 https://doi.org/10.1109/DASC-PICom-CBDCom-CyberSciTech52372.2021.00126.

Yang, J., Dong, X., Hu, Y., Peng, Q., Tao, G., Ou, Y., et al., 2020. Fully automatic arteriovenous segmentation in retinal images via topology-aware generative adversarial networks. Inter. Sci. Comput. Life Sci. 12, 323–334. https://doi.org/10.1007/s12539-020-00385-5.

Zamperini, A., Giachetti, A., Trucco, E., Chin, K.S., 2012. Effective features for artery-vein classification in digital fundus images. 2012 25th IEEE Int. Symp. . Comput. -Based Med. Syst. (CBMS) 1–6. https://doi.org/10.1109/CBMS.2012.6266336.

Zhang, J., Dashtbozorg, B., Bekkers, E., Pluim, J.P.W., Duits, R., ter Haar Romeny, B.M., 2016. Robust retinal vessel segmentation via locally adaptive derivative frames in orientation scores. IEEE Trans. Med Imaging 35, 2631–2644. https://doi.org/10.1109/TMI.2016.2587062.

Zhao, J., Ai, D., Huang, Y., Song, H., Wang, Y., Yang, J., 2019. Quantitation of vascular morphology by directed graph construction. IEEE Access 7, 21609–21622. https://doi.org/10.1109/ACCESS.2019.2895865.

Zhao, Y., Xie, J., Su, P., Zheng, Y., Liu, Y., Cheng, J., et al., 2018. Retinal artery and vein classification via dominant sets clustering-based vascular topology estimation. In: Frangi, A.F., Schnabel, J.A., Davatzikos, C., Alberola-López, C., Fichtinger, G. (Eds.), Medical Image Computing and Computer Assisted Intervention – MICCAI 2018. Springer International Publishing, Cham, pp. 56–64. https://doi.org/10.1007/978-3-030-00934-2_7.

Zhao, Y., Liu, Y., Xie, J., Zhang, H., Zheng, Y., Zhao, Y., et al., 2020. Retinal vascular network topology reconstruction and artery/vein classification via dominant set clustering. IEEE Trans. Med Imaging 39, 341–356. https://doi.org/10.1109/TMI.2019.2926492.

Zhuo, Zhang, Feng, Shou Yin, Jiang, Liu, Wing, Kee Wong, Ngan, Meng Tan, Beng, Hai Lee, et al., 2010. ORIGA-light: an online retinal fundus image database for glaucoma analysis and research. 2010 Annual International Conference of the IEEE Engineering in Medicine and Biology. IEEE, Buenos Aires, pp. 3065–3068. https://doi.org/10.1109/IEMBS.2010.5626137.